Department of Biochemistry, Faculty of Science
Charles University in Prague

Diploma Thesis

The Influence of Individual Mutations in HIV Protease on Reduced Susceptibility to the Protease Inhibitor Lopinavir

by

Klára Šašková

Supervisor: Doc. RNDr. Jan Konvalinka, Csc.

Institute of Organic Chemistry and Biochemistry
Academy of Sciences of the Czech Republic

Prague 2006

Prohlašuji, že jsem tuto diplomovou práci vypracovala samostatně pod vedením školitele Doc. RNDr. Jana Konvalinky, Csc. a všechny použité prameny jsem řádně citovala.

V Praze, dne 28.04.2006

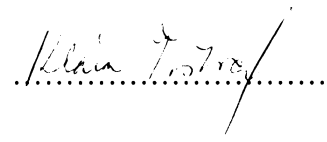

ACKNOWLEDGEMENTS

I wish to thank Jan Konvalinka for his generous arrangement of working conditions for me in his laboratory, precious advice, and a lot of astounding coffee-stories. I am also especially grateful to Milan Kožíšek for his munificent and unstinting help with my project, a lot of smiles, and for his unmistakable versions of songs.

My acknowledgement also belongs to other present and former members of Jan Konvalinka´s laboratory, mainly Jana Václavíková and Jana Pokorná for their friendly help. I also thank Pavlína Řezáčová and Jiří Brynda for introducing me to the mystery of protein crystallography.

Last but not least thanks belong to my family for their support and patience…

CONTENTS

I. Introduction

Acquired immunodeficiency syndrome (AIDS) has become one of the largest epidemies in recorded history. According to the World Health Organization, 3,1 million people died in 2005 alone, and 4,9 million people were newly infected with the human immunodeficiency virus (HIV) during the same year. Even though billions of US dollars are spent each year for the research of new antivirotics, vaccines, and health education, the mortality rate and rate of infection are still alarming.

Inhibitors of HIV protease (PI) are so far the most effective drugs that are at our disposal. Their introduction in 1995-1996 and the application of highly active antiretroviral therapy (HAART) lead to decreased mortality and prolonged life expectancy of HIV-positive patients. However, the selection pressure of virostatics leads to rapid selection of viral variants resistant towards a specific inhibitor. Different PIs select different patterns of mutations. This rapid development of resistant PR variants still remains the major problem in AIDS therapy.

Lopinavir is a second generation PI that was rationally designed to inhibit resistant PR species and is considered an important salvage drug. Even though it has been used 5 years already, its resistance profile has not been clearly defined. Mutations at 11 amino acid positions in the PR coding region were identified as associated with reduced susceptibility and were termed the "lopinavir mutation score". However, the precise role of each mutation has not been experimentally examined yet. A well-defined lopinavir resistance profile may provide insights into patient therapy and/or design of new inhibitors.

In the presented thesis, we set out to identify the relative contributions of the mutations to the lopinavir-resistance phenotype by creating a panel of resistant PR species, based on a highly resistant specimen from a patient. The mutations were introduced into the PR coding region individually or in combination in order to match the ideal "lopinavir mutation score" in the patient, who was treated by lopinavir for a prolonged period of time. Individual recombinant PRs were expressed, purified, and characterized and their inhibition profiles were analysed with a panel of PIs.

II. Current State of the Research Field

1. HIV Morfology, Life Cycle and Genome

Acquired Immunodeficiency Syndrom (AIDS) killed more than 25 million people since it was first recognized in 1981 and thus it has become global health problem. The number of people living with HIV is still growing and by the end of 2005, more than 40 million people have been infected [1].

The Human Immunodeficiency Virus HIV, the causative agent of AIDS, was first identified in 1983 [2,3]. It is a lentivirus which belongs to the family of retroviruses (*Retroviridae*), whose genome is encoded in RNA. HIV-1 and HIV-2 are two types of viruses associated with AIDS. They exist in many variants, known as subtypes,whose incidence is typical for the specific world area and their genomes are about 40% identical.

CD4+ helper T-lymphocytes are the most often attacked cells. However, B-cells, macrophages and monocytes can also be infected. The mature viral particle is schematically shown in *Figure 1.*

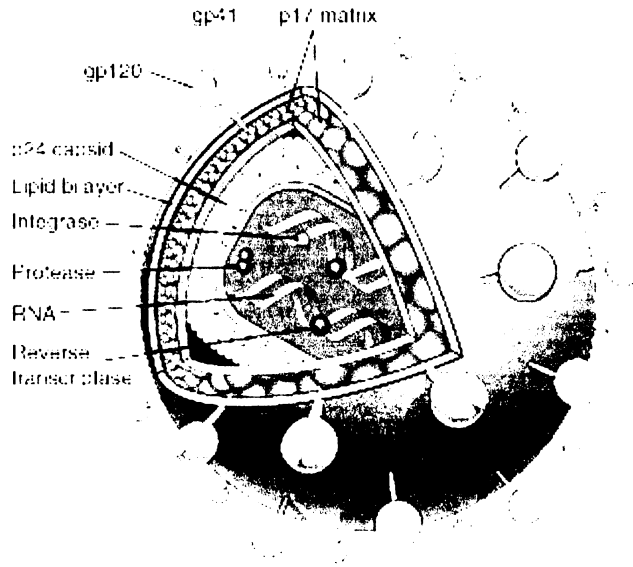

Figure 1: **HIV viral particle.** For details, see text. Reproduced from [4].

Whole virion has about 100 nm in diameter and is spherical in shape. The envelope comes from the cell lipid bilayer membrane and besides proteins from the host cell, it incorporates the envelope protein gp120 and the memrane-spanning protein gp40, that are

involved in virus entry. Matrix protein (MA, p17) forms the inner surface of the viral membrane, while the centre of the virus is made up from capsid protein (CA, p24) and forms conical capsid core. The capsid particle encapsidates two copies of viral RNA stabilized by nucleocapsid protein (NC, p7), and also contains three essential virus-encoded enzymes: protease (PR), reverse transcriptase (RT) and integrase (IN). Virus particles also package the accessory proteins: Nef, Vif and Vpr [5].

General features of the HIV life cycle are shown in *Figure 2*. There are two distinct phases: the early phase begins with viral entry, continues through the uncoating and reverse transcription and ends with the integration of the viral cDNA into the cell genome, whereas the late phase refers to the expression of viral genes and maturation.

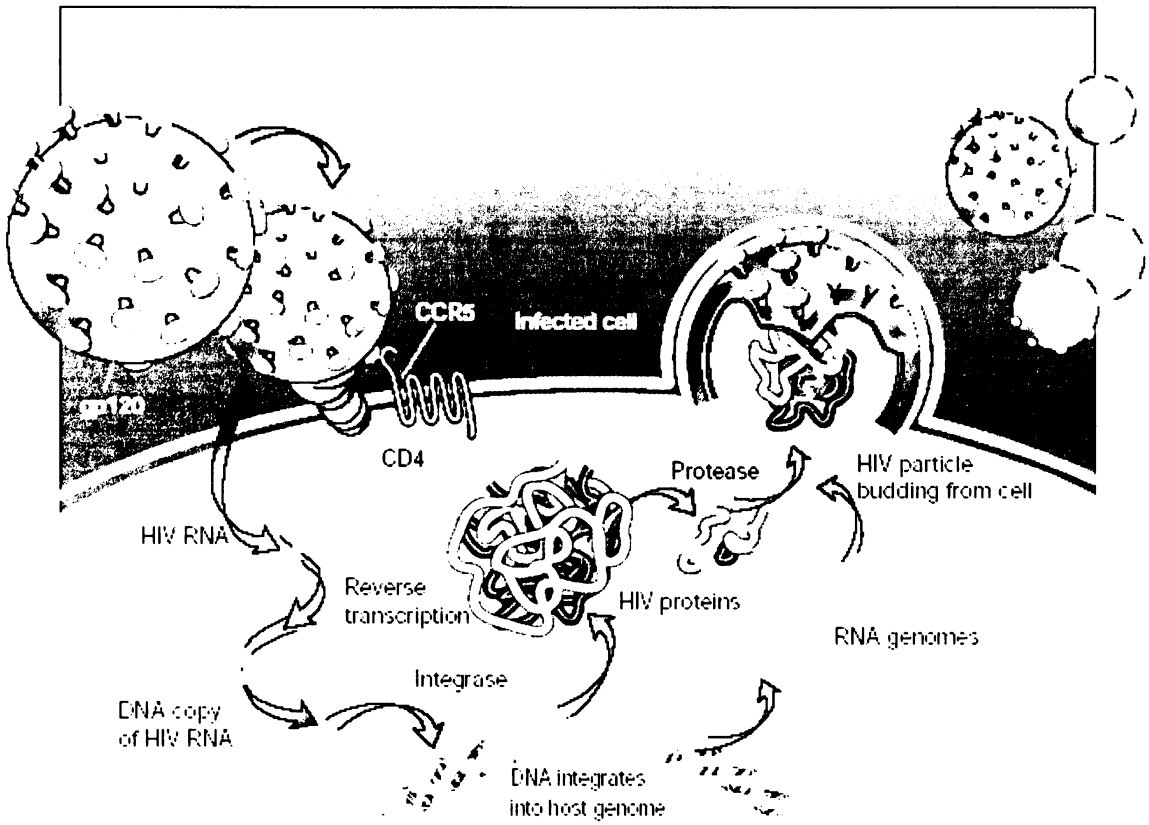

Figure 2: **The replication cycle of HIV**. For details, see text. Reproduced from [6].

HIV viral entry is a complex of multi-step mechanism that finaly enables HIV penetrate the target cell. Envelope glycoproteins gp41/gp120 as well as chemokine coreceptors CXCR4 and CCR5 are involved in the process. However, HIV can also enter target cell by direct fusion so called endocytosis, which represents alternative entry pathway [7]. The

fusion of viral and cellural membranes delivers viral RNA into the cytoplasm, where it is transcribed by the virion-packaged reverse transcriptase into the proviral dsDNA and consequently transported to the nucleus and incorporated into the chromosomal DNA of the host cell by integrase.

The late phase of the virus life cycle begins with the synthesis of unspliced and spliced mRNA transcripts produced by cellular RNA polymerase II. Unspliced mRNA is packaged into the new virions in two copies and it functions as new viral genome, while spliced mRNA serves as a template for the translation of viral genes, which is provided by the cellular ribosomes in cytoplasm. Proviral mRNA is thus translated into large polyprotein precursors: 55kDa Gag and 160 kDa Gag/Pol. The Gag protein is synthesized from the full-length viral RNA, however Gag/Pol polyprotein is a result of a -1 frame-shifting events, which allows the translation to continue in the -1 reading frame. The shiffting frequency is about 5% [8]. The spliced proviral mRNA is translated into envelope proteins: primarily in the form of gp160 precursor, which is glycosylated and subsequently cleaved by cellular serine protease into the surface protein (gp120) and transmembrane protein (gp41) [9].

Both Gag and Gag/Pol precursors, together with genomic RNA and other auxiliary proteins, assemble in lipid rafts and form the immature viral particles, that bud off from the cell [10]. During budding or shortly after budding, the viral protease cleaves the Gag and Gag/Pol polyproteins into mature products. This last step of the HIV life cycle, so called maturation, is essential for the production of infectious viral particles [11].

HIV genome consists of two copies of 9,2 kb long single strand RNA of positive polarity. The scheme of HIV-1 genomic structure is shown in *Figure 3*. At the ends of proviral DNA integrated in the host genome, long terminal repeats (LTR) are located. These non-coding sequences participate in proviral integration and subsequent transcription by cellular RNA polymerase II [12]. Three structural proteins are encoded by *gag* (p55) gene: matrix (p17, MA), capsid (p24, CA) and nucleocapsid protein (p7, NC). *Pol* encodes all viral enzymes represented by the protease (p11, PR), reverse transcriptase (p66/p51, RT), RNAseH (p15) and integrase (p32, IN). Finally *env* gene encodes the envelope glycoproteins: surface protein (gp120, SU) and transmembrane protein (gp41, TM) [13]. Further six regulatory proteins are coded in HIV genome: *tat, rev, nef, vif, vpr*

and *vpu*. They participate in viral replication and maturation. For more information, see [14].

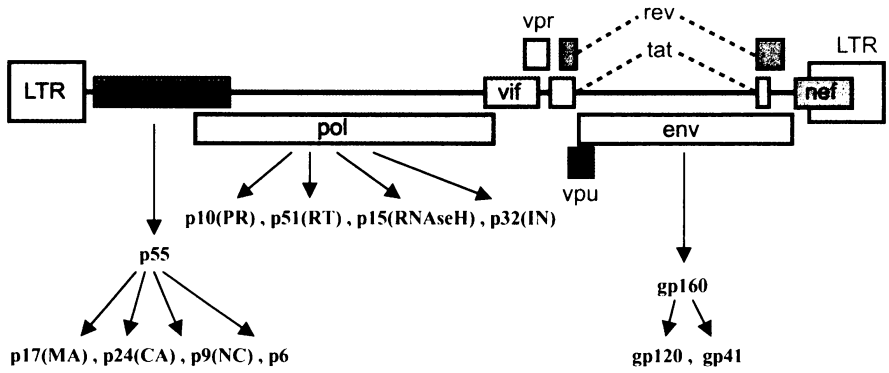

***Figure 3*: Organization of the HIV-1 genome.** The product of gag gene is cleaved by viral protease into: matrix (p17, MA), capsid (p24, CA), nucleocapsid (p9, NC) and p6 structural proteins. *Pol* encodes viral enzymes protease (p10, PR), reverse transcriptase (p5, RT), RNAseH (p15) and integrase (p32, IN). Finally *env* (gp160) encodes the structural envelope glycoproteins: surface (gp120) and transmembrane protein (gp41).

2. Structure and Function of the HIV Protease

HIV protease has the crucial role in the late steps of retroviral replication and that is why it has become one of the major targets in antiretroviral therapy. It autoactivates itself by mechanism yet undiscovered during budding or shortly after budding and subsequently cleaves the Gag and Gag/Pol polyproteins at nine processing sites into mature proteins [15]. Inactivation of the protease leads to the production of immature viral particles, that are unable to replicate and thus they are noninfectious [16].

It was supposed already from the nucleotide sequence analysis of the HIV genome, that HIV protease belonged to the aspartic acid family (aspartic protease) [17]. The notion was confirmed by site-directed mutagenesis of the putative active site aspartate (Asp25) that abolished enzyme activity; by the enzyme inhibition by pepstatin – typical aspartic protease inhibitor and finally by X-ray structure analysis of native HIV protease [18]. The aspartic protease family includes well-known enzymes like pepsin, cathepsin D, renin and chymosin [16] and the presence of highly conserved catalytic triad Asp-Thr-Gly in the active site is typical for them. The pH optimum of the HIV protease is in the range of 5,5-6,0 [15].

2.1 Enzymatic Characterization of HIV Protease

The natural cleavage sites of the HIV protease in Gag and Gag/Pol polyproteins display low sequence homology. As shown in *Figure 4,* the protease is able to cleave a variety of peptide sequences. It can also cleave other non-viral proteins (actin, calmodulin, vimentin, desmin, troponin C, ribonuclease A, etc.), hence it is toxic for the host cell [19]. The active site is formed by two identical monomers of HIV protease and it consists of 8 substrate binding pockets (S1 to S4 and S1' to S4' according to Schechter and Berger). Accordingly, the coresponding amino acid residues of the substrate bound to these subsites are marked as P1-P4 and P1'-P4'. Although there is broad variability within the amino acid residues surrounding the scissile bond, there seems to be a pattern represented by conformational factors (hydrophobic/hydrophilic interactions, polarity, surface and secondary structure of the substrate). There are few general rules that should be considered: substrates are at least seven residues in length (P4 – P3') [19], aromatic or hydrophobic residues are preferred in P1/P1', Glu of Gln is often in position P2', while in position P2 are often hydrophobic residues. In P1 – P2' Lys never occurs [19, 20]. Large residues could be found in P3, Glu is usually in P3', P2' or P4 prefers small hydrophilic residues.

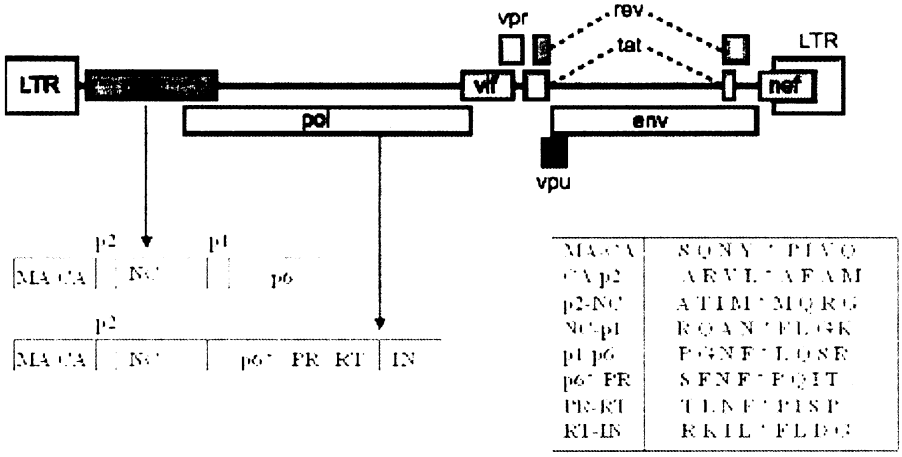

Figure 4: **HIV polyproteins and natural cleavage sites of HIV-PR.** The amino acid sequences are in the one-letter code; * indicates the scissile bond. The cleavage site within the RT is not shown.

2.2 Three-Dimensional Structure of HIV Protease

HIV protease is one of the best-understood enzyme regarding structure-function relationship, for it represents an important pharmaceutical target and a correspondingly significant object of X-ray crystallography.

As shown in *Figure 5,* HIV protease is a dimeric and symetric molecule that consists of two identical 99-residue subunits. The two monomers of the homodimer are related to each other by a 2-fold rotation axis and they interact through the β-sheets formed between two N- and C- termini (residues 1-4 and 96-99) of each monomer (*Figure 5C*).

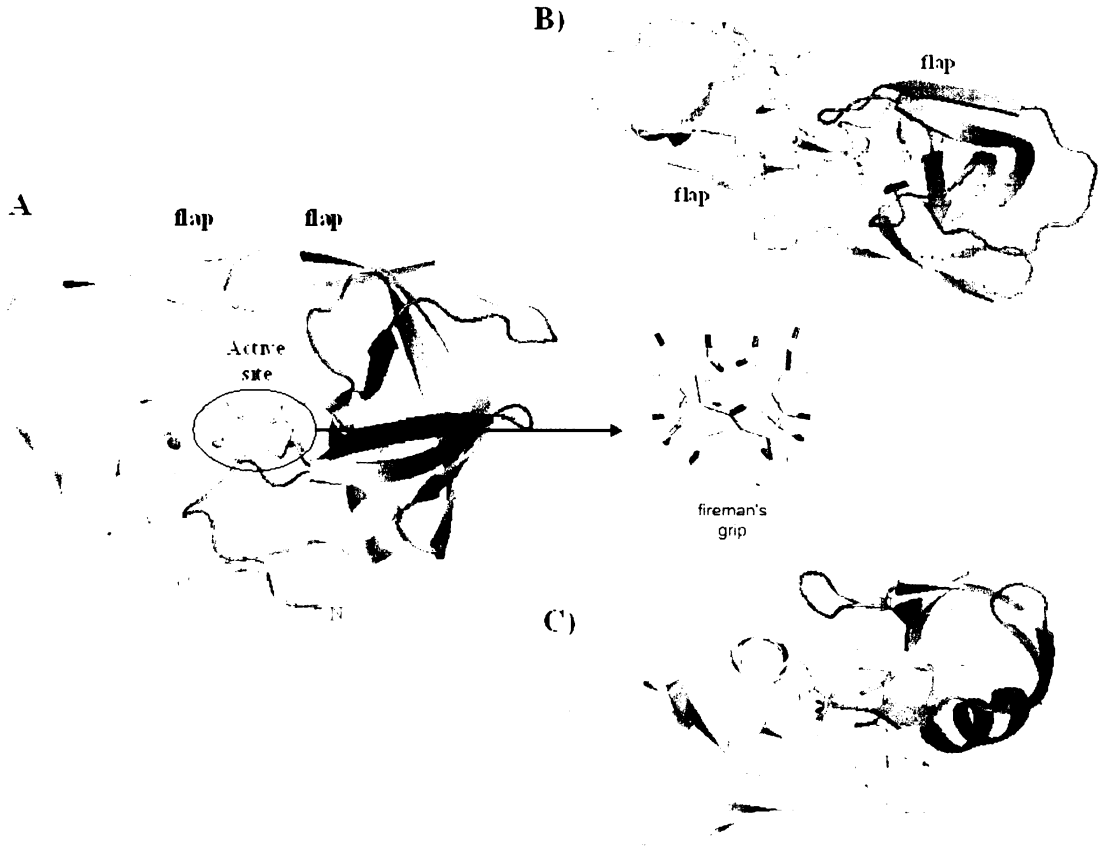

***Figure 5*: Three-dimensional structure of HIV-1 protease.** (A) Overall view into the active site. Two monomers are shown in yellow and violet, the active site aspartic acid residues are shown in stick representation at the bottom of the active site. Detailed view of „fireman's grip" is also shown. (B) Top view along the 2-fold axis showing flaps above the active site. (C) Bottom view along the 2-fold axis showing the dimer interface. The figure was created using program PyMOL 0.98 [21] from the structure determined by Stoll et al., 2002 (PDB entry 1 MUI) [22], the inhibitor bound to the active site is not shown.

These interactions improve the stability of the dimer [23]. The active site region is made up of contributions from a number of residues, however the major effect of the proteolytic cleavage reaction has the catalytic triad forming the „fireman´s grip". It is formed by ...Asp25-Thr26-Gly27...residues and it is situated at the bottom of the cavity within the loop that forms a network of hydrogen bonds with the corresponding loop of the oposite monomer [24]. The constellation of the active site represents by two carboxyl groups from the Asp25 residues is similar to that seen in many aspartic proteases.

Two flexible flaps play an important role in substrate binding (Ile47-Gly-Gly-Ile-Gly-Gly52). They remain in the open conformation (7Å distant from the active site), but upon binding of substrate or inhibitor, they close the cavity and interact tightly with the bound compound [25]. Another important structural feature in the HIV PR is the dimerization domain formed by N- and C- termini of each monomer as mentioned above. These intramolecular interactions are very strong (involving number of hydrogen bonds) and it is known that peptides mimicking these terminal segments inhibit protease by disruption of the dimer structure [26]. This suggests an alternative approach to inactivate the enzyme.

3. The HIV Protease as a Pharmaceutical Target

The first effective drug against HIV was the reverse transcriptase inhibitor azidovudin (AZT), which was originally developed as an anticancer drug. But it was identified by screening of huge numbers of coumpounds already produced for other purposes. Therefore, there was a need for more sophisticated approach, a structure based drug design. The prototype of this approach was the expression, purification and crystallization of the HIV protease-enzyme that plays important role in viral maturation. Protease inhibitors (PI) - a class of antiretroviral drug - were first approved by the FDA in 1995 [27] and to this date, there are nine PIs on the market. Due to such an interest, HIV protease is now one of the best characterized enzymes.

The approval process of any drug is very complex. The ideal HIV PR inhibitor must fulfil a number of qualities, for instance: the drug needs to bind HIV PR with high afinity (K_i in subnanomolar range); it should also show high specificity; it must be active

against large spectrum of viral isolates and the drug should have good oral bioavailability in humans.

3.1 Clinically Used Inhibitors of HIV Protease

Saquinavir (SQV, Ro 31-8959), developed by Hoffmann-La Roche, was the first PI to undergo clinical evaluation. It is a highly active peptidomimetic PI incorporating the hydroxyethylenamine isoster and it is currently distributed in three different forms (all marketed by Hoffmann-La Roche) [24]. The hard-gel capsule form of saquinavir (Invirase) was approved by FDA in 1995. However, these capsules are poorly absorbed and thus the drug levels are too low to achieve active antiviral activity. The soft-gel capsules, that were approved by FDA in 1997 and are known as Fortovase, allow adequate absorption. Finally, the tablet form was approved in 2004 for using in combination with low-dose ritonavir, another clinically used PI [28].

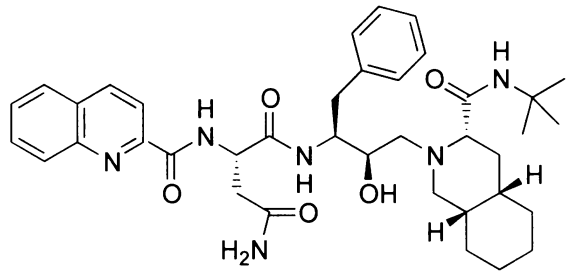

Figure 6: **Chemical structure of saquinavir**

Ritonavir (RTV, ABT-538), developed by Abbott Laboratories, was the second HIV PI to be licensed in the USA (1996) and it is known as Norvir in clinical use. Ritonavir is derived from C2-symetric peptidomimetic inhibitor [29], however, its final structure is asymmetrical. It show some problematical side effects, nevertheless, it was shown that this compound is a potent inhibitor of cytochrom P-450. Therefore ritonavir is widely used to enhance effect of other PIs, that are metabolized via cytochrom P-450 metabolic pathway.

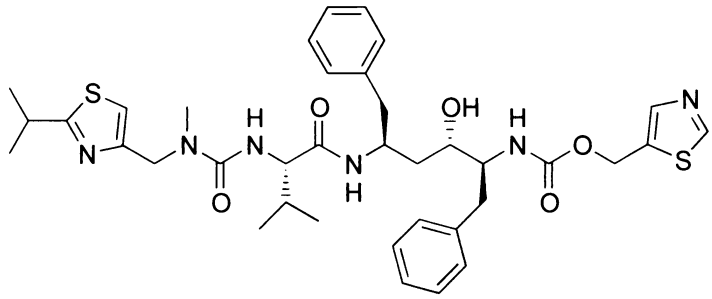

***Figure 7*: Chemical structure of ritonavir**

Indinavir (IDV, MK-639) was designed by Merck & Co., approved by FDA in 1996 and marketed as Crixivan. The drug also acts as peptidomimetic transition state analogue and belongs to the class of PIs known as HAPA (hydroxyaminopentane amide) compounds [30].

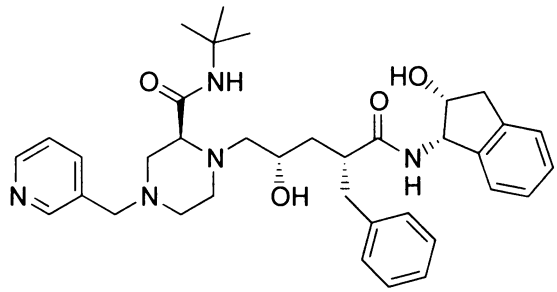

***Figure 8*: Chemical structure of indinavir**

Nelfinavir (NFV, AG-1343), developed by Agouron Pharmaceuticals, was approved by FDA in 1997 and marketed as Viracept. It is a selective, nonpeptidic PI that was designed by protein structure-based techniques using X-ray analysis [31]. Nelfinavir was the first PI that recieved the FDA approval for the treatment of children. It is well absorbed and disposes only slight side effects.

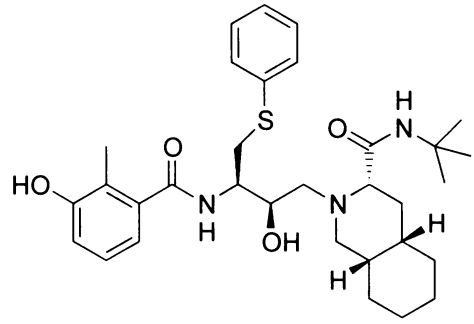

***Figure 9*: Chemical structure of nelfinavir**

Amprenavir (APV, 141W94 or VX-478) was developed by Vertex Laboratories (now GlaxoSmithKline) and approved by FDA in 1999 marketed as Agenerase. It belongs to the class of sulfonamid PIs and it was designed by using X-ray crystallographic data of the enzyme [32]. Another PI developed by Vertex Laboratories in colaboration with GlaxoSmithKline is fosamprenavir (fAPV, GW 433908, VX-175) [33,34]. As seen in *Figure 9*, it is an phosphate ester of amprenavir, that proved to have better pharmacokinetic properties.

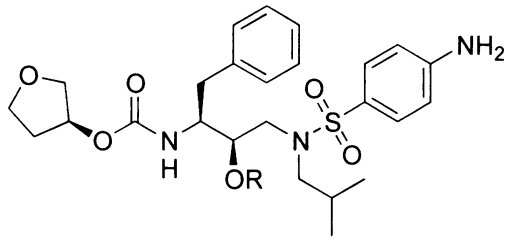

Figure 10: **Chemical structure of amprenavir and fosamprenavir.** R=H (APV) and R= $P(0)(0H)_2$ (fAPV)

Lopinavir (LPV, ABT-378) was developed by Abbott Laboratories as the first second-generation inhibitor, approved by FDA in 2000. It was designed by using the X-ray crystal structure of the complex of HIV-1 PR and ritonavir, thus primary against the mutation Val82 in the active site of the enzyme that mutates in response to ritonavir therapy [35]. Paradoxically, Val82 belongs to mutations increasing lopinavir resistance. It is marketed as Kaletra, which also involves small amount of ritonavir to improve its pharmacokinetic profile.

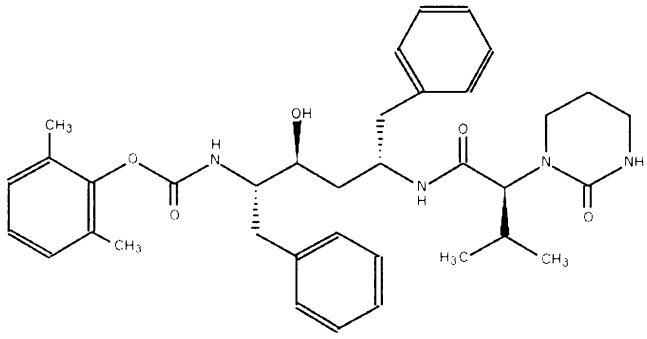

***Figure 11*: Chemical structure of lopinavir**

Atanazavir (ATV, BMS-332632, CGP 73547) was also developed by using structural studies. It is marketed as Reyataz by Bristol-Myers Squibb and was approved by FDA in 2003 [36]. It enables once-daily dosing, which is better tolerated by patients.

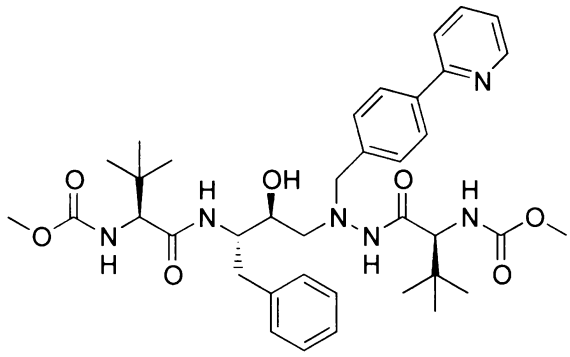

Figure 12: **Chemical structure of atazanavir**

Recent FDA approval (June 2005) received a nonpeptidic inhibitor **tipranavir** (TPV, PNU-140690) designed in Pharmacia and further developed by Boehringer Ingelheim Pharmaceuticals, Inc., marketed as Aptivus. It is intended to be used as part of combination therapy in patients who have HIV strains resistant to other PIs [37].

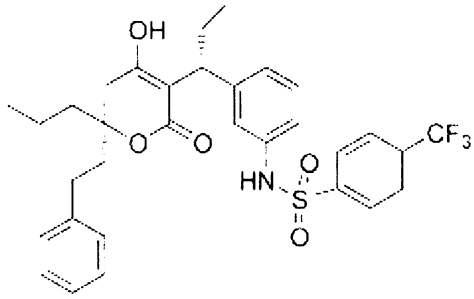

Figure 13: **Chemical structure of tipranavir**

3.2 Drug Resistance and HIV Protease Inhibitors

HIV resistance is an increasingly complicated phenomenon. The introduction of antiviral therapy has had a dramatic effect on the natural behaviour of HIV. The virus in plasma is composed of a mixture of numerous quasispecies [38], which is partly due to the high error rate of HIV reverse transcriptase as well as the absence of proofreading mechanism. This natural genetic diversity of HIV increases by using antiviral drugs, that significantly reduce morbidity and mortality associated with HIV infection. However, incomplete suppression of the virus and selection pressure leads to larger amount of

genetic variants. Resistance to PIs usually begins with a single mutation involving the active site of the virus and can be observed in weeks of therapy. Ongoing replication under selective drug pressure leads to the accumulation of additional mutations across the gene that increase viral fitness and also promote cross-resistance to other PIs [39].

3.2.1 Determination of the Resistance – Resistance Assays

Due to the increased prevalence of HIV drug resistance and also transmission of resistant virus, HIV resistance testing has become a key component of HIV patient management. It is also highly recomended to HIV infected pregnant women to optimize treatment and prophylaxis of the neonate. Many laboratory tests have been developed and validated to assist in recognizing HIV resistance. They are based on either genotyping or phenotyping characteristics.

A genotype assay involves either the full examination of the particular genetic sequence (protease, reverse transcriptase, cleavage sites) or point hybridization assays to identify resistance-associated mutations [40, 41]. The assays are available as a kit and some of them in a form of commercial service. Chip hybridization assays (Roche Molecular Systems, BioMerieux) are more easy to use than sequencing methodologies, but they are less flexible in terms of incorporation of additional newly identified mutations. Better understanding of the relationship between genotype (resistance mutations) and phenotype (biological characteristics, i.e., sensitivity of a given mutant to a given PI) still remains the challenge. There are softwares approved by FDA using genotype for predicting phenotype: the group of mutations identified from the viral genetic sequence is compared with database of samples that have been both phenotyped and genotyped [42]. So far these programs revealed satisfying correlation between the virtual phenotype and actual phenotype.

Phenotyping is an assessment of the ability of the virus to replicate in the presence of various concentrations of tested drug. The most common method today is recombinant viral assay (RVA) where relevant amplified section of HIV genome are inserted into a vector to make a replicating recombinant virus. This recombinant virus is then allowed to grow in various concentration of tested drug [43]. IC50 (concentration of the inhibitor required to inhibit 50%) is determined and compared with the value of the wild type to

calculate a fold change in IC50. Reduced susceptibility was defined as greater than 2,5-fold change (Virologic) or greater than 4-fold change (Virco) in IC50. These two assays correlate with each other in 92% [44]. Beside phenotypic assays reguired recombinant virus, *in vitro* enzymatic assay may be also used to assess susceptibility of the virus to the given inhibitor. This method will be further described in chapter IV.7.

3.2.2 Resistence to Clinically Used Protease Inhibitors

The resistance to protease inhibitors is connected with specific modifications in the protease structure, called resistance profile, which is characteristic for particular drug. A recent survey revealed that there can be up to 49 amino acid changes in HIV-1 PR, which comprises more than half of the total 99 residues [45].

There are generally two types of mutations that arise in HIV PR, classified as either primary or secondary mutations. The primary mutations are those selected first in the presence of the drug and they are also very specific for each inhibitor. In general, these mutations tend to be the primary contact residues for drug binding, they alter the binding of the drug and thus directly affect the drug susceptibility phenotype. Obviously, they occur in the active site of the enzyme and since the first primary substitution (V82A) has been identified, several of the active site amino acid residues were shown to mutate in response to drug therapy [46]. The secondary mutations mostly emerge later than primary mutations, and by themselves they mostly do not have a significant effect on phenotype. However, in some cases, they can indirectly influence the inhibitor binding via long-range structural perturbations of the active site or they can change the stability of the enzyme. Moreover, this category involves so called compensatory mutations, that can improve replicative fitness of virus already containing primary mutations [47].

Besides mutations in the protease gene, the viral susceptibility to PIs may be altered by mutations in cleavage sites. They are compensatory rather than primary and so far there have been no reports that changes in the cleavage sites alone can cause PI resistance. The most frequent changes were observed at the cleavage sites in the 3′ part of the *gag* gene-p7/p1 and p1/p6, mainly during the treatment with indinavir, amprenavir and lopinavir [48].

Apart from all those three mechanisms mentioned above, other possible way how to escape the drug pressure was recently identified. It is represented by amino acid insertion in the protease gene, usually at positions 18, 25, 36, 70 and 95 [49].

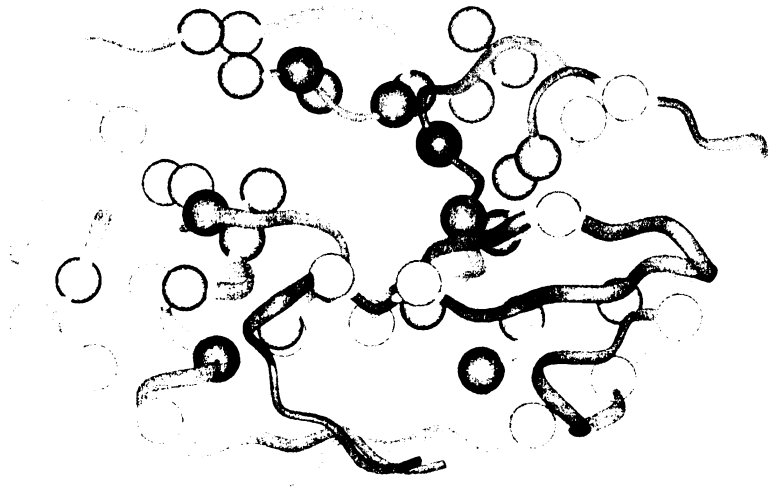

Figure 14: **Resistance mutations in HIV PR.** Primary mutations are shown in red; secondary mutations in green and those with the compensatory effect are marked in yellow. The figure was created by Martin Lepšík from IOCB AS CR.

Mutations in the protease gene associated with resistance to PIs are summarized in *Figure 15*. Primary mutation selected during saquinavir therapy is either G48V or L90M. They are slightly occuring together *in vivo* and both show cross-resistance to other PIs. Amino acid residue 48 is in the flexible flap loop and G48V substitution can result in less conformational freedom and greater rigidity of the flap. Residue 90 is located outside the binding pocket of the enzyme and L90M mutation may induce conformational perturbations in the enzyme altering binding of the inhibitor [50]. In the case of nelfinavir, two evolutionary pathways driving the resistance have been shown. As the first mutation, D30N or, less frequently, L90M exchange occur [51,52]. Viral species with these substitutions combined are very rare. I50V is primarily selected during amprenavir therapy and, surprisingly, it increases viral susceptibility to other PIs [53]. Mutations V82A/T/F/S and I84V occur in patients treated with indivavir and ritonavir or amprenavir and atanazavir, respectively, and both confer high level of cross-resistance to all clinicaly used PIs (see *Figure 15*).

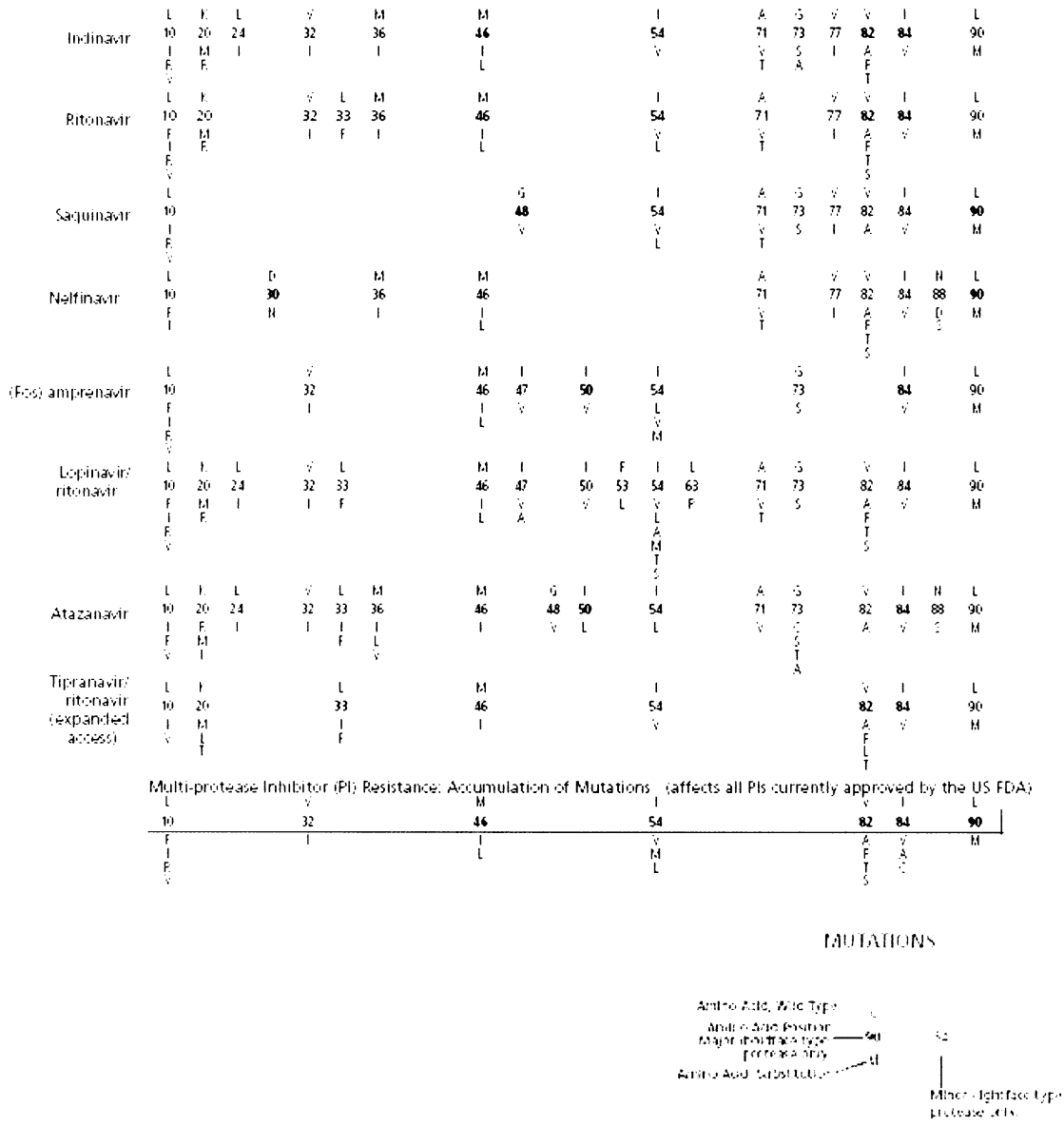

Figure 15: **Mutations in the protease gene associated with resistance to PIs.** For details see text. Reproduced from [51]

3.2.3 New Drugs and Approaches

Drug discovery process during the HIV/AIDS therapy revealed an indisputable success of the rational drug design. This structure-assisted drug design utilizes techniques such as protein crystallography, nuclear magnetic resonance (NMR), advanced chemical

synthesis and computational chemistry [54]. However, these advanced techniques are still combined with traditioanal serendipity methods based on random testing of compound libraries. Combination of these different appoaches can lead to unexpected structures, that will possibly show better bioavailability and stability, less side effects and not so rapid developement of resistant viral strains.

One of these unconventional compounds and a promising candidate for a novel class of nonpeptidic PIs is a class of boron containing compounds called metallacarboranes. They are specific and potent inhibitors of HIV protease. *Figure 16B* shows the most active compound, sodium hyfrogen butylimino bis-8,8-[5-(3-oxa-pentoxy)-3-cobalt bis(1,2-dicarbollide)]di-at. This inhibitor exhibits a K_i value of 2,2 nM and a submicromolar EC_{50} in antiviral test. The structure of parent compound cobalt bis(1,2-dicarbollide) in complex with HIV PR is also shown (*Figure 16A*). Most of the metallacarboranes are chemicaly and biologicaly stable, some of them show low toxicity and they could be modified in various ways [55]. These characteristics make them attractive pharmacophores.

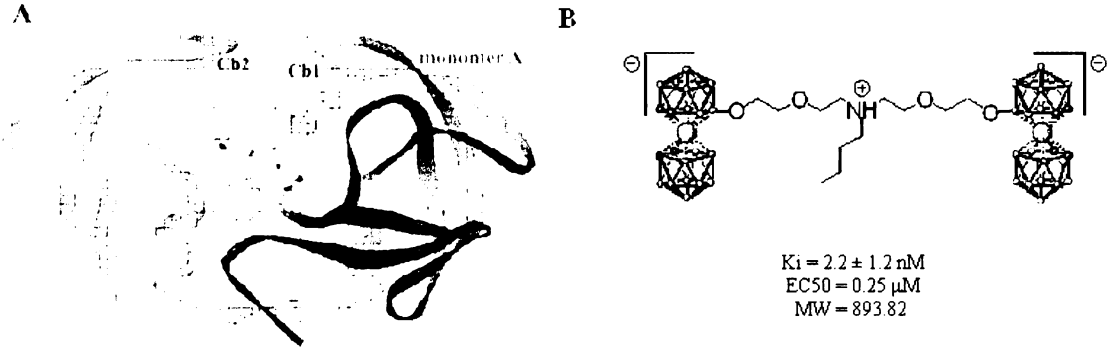

Figure 16: **Structures of metallacarboranes.** (A) Overall structure of cobalt bis(1,2-dicarbollide) in complex with HIV PR. (B) Structure and activity of most potent metallacarborane PI. Reproduced from [55].

4. Lopinavir and its Resistance Profile

Lopinavir is an example of the successful application of rational drug design. As already mentioned in chapter 3.1, this protease inhibitor was developed by Abbott Laboratories, the same company that previously introduced another potent PI ritonavir into

clinical practice. The main intention at the beginning of new drug discovery was simple: to achieve better qualities where ritonavir has limped, while keeping the good ones.

Ritonavir is a PI with high oral bioavailability and long plasma half-life. However, the *in vitro* antiviral activity of ritonavir is attenuated by 20-fold in the presence of human serum. Futhermore, monotherapy with ritonavir selects resistant viral isolates with primary mutation at position 82. The selection of Val82 mutants with reduced affinity for the inhibitor is consistent with the hydrophobic interaction between ritonavir and the isopropyl side chain of Val82. Lopinavir was thus originally designed to diminish these interactions [35].

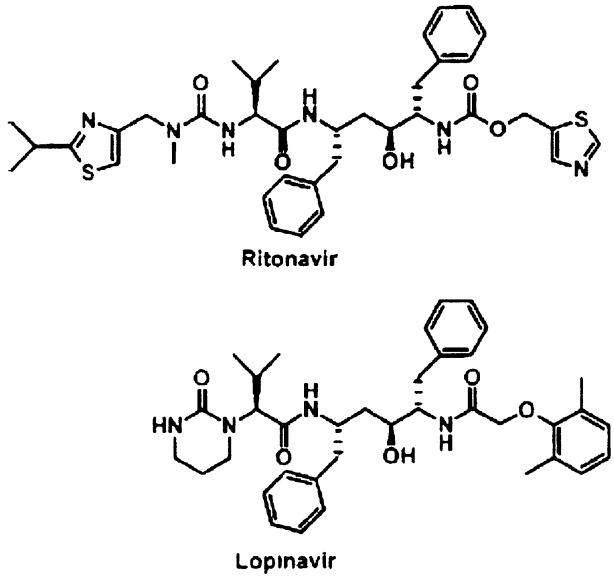

Figure 17: **Chemical formulas of ritonavir and lopinavir**

As seen in *Figure 17* the core of lopinavir is identical to that of ritonavir. The 5-thiazolyl end group in ritonavir was replaced by the phenoxyacetyl group, and the 2-isopropylthiazolyl group in ritonavir was replaced by a modified valine in which the amino terminus had a six-membered cyclic urea attached. These modifications of parent ritonavir structure led to promising pharmaceutical properties. Lopinavir inhibits wild-type HIV-1 PR with Ki value 1,3 pM and it is also active againts the V82A, V82F and V82T mutant proteases. Moreover, in the presence of human serum, lopinavir is 10-fold more potent than ritonavir [35]. Despite these advantages, the plasma level of lopinavir decreases very quickly in humans. The observation that ritonavir significantly elevates the concentrations of other PIs in plasma through inhibition of their cytochrom P-450-mediated metabolism

was used for two drugs coadministration. In the presence of subclinical amounts (50 mg) of ritonavir, lopinavir concentration could be maintained for over 24 h after a single 400 mg dose [56].

The structure of the complex of HIV-1 PR with lopinavir (*Figure 18B*) revealed novel hydrogen bonding arrangement with Asp29 of the enzyme and the cyclic urea unit of the inhibitor. This interaction is shown in *Figure 18A*. The urea carbonyl of

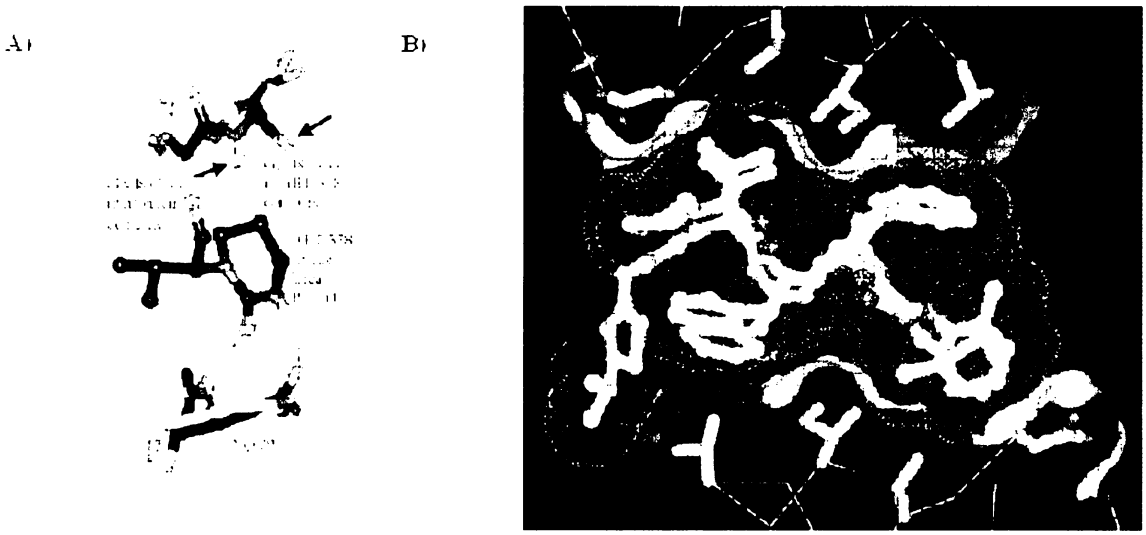

Figure 18: (A) H-bond interactions between the terminal P_2 cyclic urea unit of LPV and Asp29 and VdW contacts of the trimethylen portion of this unit with Gly48. LPV is shown in black, while RTV is shown with white carbons. (B) Active site of LPV (white carbon atoms with white dotted surface) and RTV (blue carbon atoms with blue dotted surface) in HIV-1 PR. The protein surfaces of Val82 and its C_2-symmetrical partner residue are colored red to indicate the region of resistance in V82 mutants. Reproduced from [22].

LPV accepts a hydrogen bond from the backbone N-H of Asp29, and the terminal urea N-H donates a hydrogen bond to the sidechain of Asp29. Subsequently, slight shift in the protein backbone near Gly48 occurs. As already mentioned above, the design strategy was primarily directed to diminish van der Waals interaction with Val82 of the enzyme and ritonavir. This goal was successfuly reached by replacing the isopropylthiazolyl group of ritonavir by the shortened cyclic urea unit of lopinavir. The comparison of the structures of lopinavir and ritonavir with HIV-1 protease are shown in *Figure 18* [22].

4.1 Lopinavir Mutation Score

The combination of two protease inhibitors lopinavir and ritonavir was approved for clinical use by Food and Drug Administration as Kaletra, and lopinavir is the first second-

generation protease inhibitor to become a drug. The typical pill combination is 133 mg of LPV and 33 mg of RTV. Kaletra is now considered an important salvage drug, which is predominantly administred after primary therapy with PIs failed.

Lopinavir like each newly approved PI was *in vitro* tested for the emergence of the drug resistance. HIV strains resistant to lopinavir have been produced using *in vitro* passaging and this analysis revealed folowing mutations in protease gene: I84V, L10F, M46L, T91S, V32I and I47V/A [57]. Additional information was achieved by observing PI-experienced patients that display *in vitro* resistance to other PIs. 112 HIV isolates were used to examine the genotypes and phenotypes to define the genotypic correlates of reduced *in vitro* susceptibility to lopinavir. This analysis showed that specific mutations at 11 amino acid positions in protease were associated with reduced susceptibility to this PI: L10F/I/R/V, K20M/R, L24I, M46I/L, F53L, I54L/T/V, L63P, A71I/L/T/V, V82A/F/T, I84V and L90M. The panel of these mutations was termed as "lopinavir mutation score" [58].

Since the relative contributions of each individual mutation has not been clearly defined yet, we decided to analyse them by *in vitro* phenotypic assay. Some of the sugestions were already made [58]: mutations at positions 82, 54, 10, 63, 71 and 84 seem to have relatively modest effect on phenotype (4- and 10-fold), while the K20M/R and F53L substitutions, in conjunction with other mutations, seem to be associated with more than 20- and 40-fold-reduced susceptibility, respectively. It is also believed that the cumulative number of these mutations shows higher level of resistance. Our aim was to examine the contribution of each mutation by *in vitro* site-directed mutagenesis that allows introducing of single mutations into the characterized backround. Well defined lopinavir resistant profile may provide insights into either patients therapy or design of new inhibitors.

III. Aims of the Study

- Amplify protease coding regions from patient samples, identify those with the highest "lopinavir mutation score" and clone them into expression vector.

- Insert additional mutations in order to reach the full "lopinavir mutation score" into the framework of patient-derived protease by site-directed mutagenesis individually or in combination.

- Express in *E.coli*, purify and enzymatically characterize protein-engineered and patient-derived HIV proteases.

- Determine the 3D structure of the most intriguing HIV-1 PRs (in term of lopinavir resistance) in complex with lopinavir and compare the overall structures to the structure of wild-type HIV-1 PR.

IV. Materials and Methods

1. Reagents and Instrumentations

1.1 List of Chemicals

- **Bio-Rad,** Hercules (USA)
  agarose, protein assay – dye reagent
- **Biosynth AG,** Staad (Switzerland)
  IPTG
- **Lach-Ner,** Neratovice (CZ)
  acetic acid, acetone, ethanol, ethyleneglycol, formaldehyde, hydrochloric acid, isopropanol, argent carbonate, sodium acetate, sodium carbonate, sodium hydroxide,sodium thiosulphate, sodium chloride, potassium acetate, calcium chloride, sodium dihydrogenphosphate, sodium hydrogenphosphate, potassium dihydrogenphosphate, diamonium hydrogenphosphate, urea
- **MBI Fermentas,** Greenland (USA)
  T4-DNA ligase, buffer for T4 DNA-ligase
- **New England BioLabs,** Ipswich (USA)
  restriction endonucleases (*EcoRI*, *NdeI* and *DpnI*), NEBuffer 2
- **Penta,** Prague (CZ)
  methanol
- **Promega,** Madison (USA)
  Pfu DNA polymerase, *Pfu* DNA buffer
- **Serva,** Heidelberg (Germeny)
  bromphenol blue, Coomassie Brilliant Blue G250, lysozyme
- **Sigma-Aldrich,** Buchs (Switzerland)
  EDTA, PEG 8000, SDS, DMSO , phenol, chlorophorm, LB Broth, LB Agar, 2-mercaptoethanol, PMSF, lithium chloride, glycerol, Ribonuclease A, N,N,N',N'-tetramethylethylenediamine, N,N'-bisacrylamide, kanamycin sulfate
- **Top-Bio,** Prague (CZ)
  dNTP's, *Taq* DNA polymerase, *Taq* DNA buffer, Coloured DNA marker 155-970
- **USB,** Cleveland (USA)
  ethidium bromide, acrylamide, glycin, TRIS, MES , HEPES

1.2 Instruments

- Thermocycler GeneAmp PCR System 2400, Perkin-Elmer (USA)
- Horizontal electrophoresis apparatus, Gibco (USA)
- UV lamp Herolab UVT-20 S/M/L (Germany)
- centrifugies: Megafuge 2.0R, Heraeus Instruments (Germany)
  Biofuge pico, Heraeus Instrument (Germany)
  Beckman J2-MI (USA)
  Hermle Z 233 Mk-2, Biotech (CZ)
- rotate incubator Innova 4300, New Brunswick Scientific (Germany)
- sonicator Soniprep 150, Sanyo (USA)
- pH meter Unicam 9450 (USA)
- autoclave MLS-3020U, Sanyo (Japan)
- spektrophotometers: UV-VIS spectrophotometer UNICAM UV 500, Prague (CZ)
  UV-VIS spectrophotometer UNICAM Helios Alpha, Prague (CZ)
- vertical polyacrylamid gel eletrophoresis, SIGMA-ALDRICH (USA)
- Vac-Man Laboratory vacuum manifold, Promega (CZ)
- ÄKTAExplorer FPLC system, Amersham Pharmacia Biotech (Sweden)
- DC 290 Zoom Digital camera, Kodak (USA)
- microskop Nikon SMZ 660 (Japan)
- Mar345 Image Plate System (Germany)
- Nonius FR591 Rotating Anode Generator (Holland)
- thermostates: Techne, Cambrige Ltd. (UK)
  Thermomix BU, B. Braun (Germany)

1.3 Other Materials

- MonoS HR5/5 FPLC Column, Pharmacia (Sweden)
- dialysis membrane Spectrapor, Spectrum Laboratories (USA)
- DNA Lego-kit , TopBio (CZ)
- PVDF membrane, Millipore (USA)

- PE Biosystems BigDye^{TM} Terminator Cycle
- Sequencing Ready Reaction kit, Perkin Elmer (USA)
- QIAquick Gel Extraction Kit, QIAGEN (USA)
- Centricon-10 devices, Millipore (USA)
- Nextal Crystallization Tool NCP-24, Nextal Biotechnologies (Canada)
- Crystal Screen Reagent formulation, Hampton Research (USA)
- Addition Screen I, Hampton Research (USA)
- nylon fiber CryoLoop, Hampton Research USA)

1.4 Bacterial Strains, Vectors and Media

- Bacterial strain *Escherichia coli* BL21 (DE3)RIL, Novagen (USA)
- Bacterial strain *Escherichia coli* DH5α , Novagen (USA)
- LB Broth, Sigma-Aldrich (Switzerland)
- LB Agar, Sigma-Aldrich (Switzerland)
- pET24a expression vector, Novagen (USA)

2. Isolation and Amplification of the Patient-derived HIV-1 PR Coding Region

Within a long-term epidemiological study, HIV-positive patients receiving highly active antiretroviral therapy (HAART) at the Faculty Clinic Bulovka in Prague have been closely followed for the presence of resistant HIV species. Selection of the patient CZ13 for this study was based on the genotyping and clinical markers suggesting resistance development to the protease inhibitor lopinavir.

There are two patient-derived HIV-1 PRs used in this study - K1 and K4. Both DNA samples have been generously provided by Jana Václavíková (laboratory of Jan Konvalinka, IOCB AV CR), who is involved in clinical studies monitoring the evolution of drug resistance with focus on HIV protease [59].

3. Generation of Recombinant PRs with PI Resistance Mutations

3.1 Amplification of the Protease Coding Region

The HIV-1 PR coding region was obtained from PCR reactions using a forward primer 5′- ATCCTTTCATATGCCTCAGATCACTTTTG- 3′ specific to the 5′-end of the PR coding region with a *NdeI* cleavage site and a reverse primer 5′- TTGAATTCGATATCATTAAAAATTTAAAGTGCAGCC- 3′ including a site for *EcoRI* and two stop codons (see *Figure 19*). Primers were designed in Jan Konvalinka′s laboratory and synthetized by Generi Biotech (CZ).

PCR mixture:

Compound	Volume
Taq buffer (10x, according to the manufacturer′s recomendations, Top-Bio (CZ))	2,5 µl
Sterile HPLC water	12,5 µl
25mM $MgCl_2$	1,5 µl
10mM dNTP	1 µl
Taq DNA polymerase	0,5 µl
Forward primer (20µM)	0,5 µl
Reverse primer (20µM)	0,5 µl
DNA template	1 µl
Mixture volume	25 µl

PCR reactions were performed in a thermocycler GeneAmp PCR System 2400 (Perkin-Elmer, USA) under following conditions:

1.) 95°C/5min

2.) (95°C/30s - 55°C/30s - 72°C/1min) 34 cycles

3.) 72°C/8min - 4°C

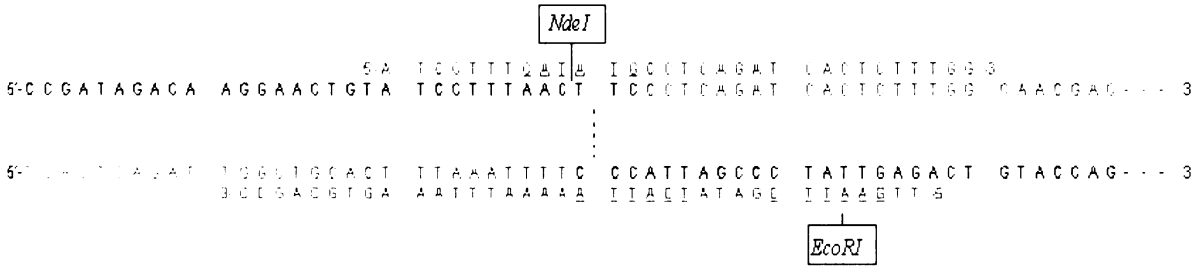

Figure 19: The beginning and the end part of the proviral DNA sequence coding HIV PR (in blue). Primers are shown in red with marked restriction sites and stop codons.

3.2 DNA Cleavage by Restriction Enzymes

A typical restriction enzyme analysis, using *NdeI* and *EcoRI* restriction endonucleases, was performed according to the manufacturer's recomendations (Top-Bio, CZ):

PCR sample	*NdeI*	*EcoRI*	NEBuffer 2	Sterile water
25µl	1,5µl	1,5µl	5µl	17,5µl

Reaction proceeded at 37°C overnight.

3.3 Horizontal Agar Gel Electrophoresis

Buffers :

TAE buffer (50x) : 242g Tris-HCl, 57,1 ml 99% CH_3COOH, 100 ml 0,5M EDTA; water to 1 liter, pH 8,0

Sample buffer : 40% (w/v) sucrose, 0,1% (w/v) bromphenol blue

PCR procedures were monitored by horizontal agar gel electrophoresis. 1,3% agar gel was prepared from 30ml of TAE buffer (1x) and 0,39g of agarose. The suspension was heated for 1 min till complete dissolution. After chilling the suspension to 60°C and refilling water to original weight, 30 µl of ethidium bromid (0,5mg/ml) were added. Before loading onto the gel, DNA samples were mixed with the sample buffer in the ratio 5:1. Electrophoresis was carried out in a horizontal electrophoresis apparatus filled with TAE

buffer (1x). Gel was run at a constant voltage of 120 volts for about 20 min. Separated DNA were detected under UV lamp (Transilluminator UVP, USA) and photographed by DC 290 Zoom Digital camera (Kodak, USA).

3.4 DNA Isolation from Agarose Gel

DNA was isolated from the agarose gel using QIAquick Gel Extraction Kit (QIAGEN, USA), buffer composition i.e. QIAquick Spin Handbook. Approximately 200mg of the gel was suspended in 600µl of buffer QG and incubated for 10 min at 56°C. 200 µl of isopropanol was added and the solution was centrifuged (10000g, 1 min). The filtrate was discarded and the membrane was washed by 0,75ml of buffer PE. Another centrifugation (10000g, 1 min), the filtrate was discarded and next centrifugation followed (10000g, 1 min). Finally, the column was transferred into a microtube and by addition of 50 µl of sterile water and following centrifugation (10000g, 1 min) the DNA was eluted.

3.5 Ligation of the HIV-1 PR Coding Region into the Expression Vector

DNA isolated from the agarose gel was ligated into the expression vector pET24a, which had been cleaved before by *NdeI* and *EcoRI* restriction endonucleases.

A typical ligation reaction was performed according to the manufacturer's recomendations:

DNA isolated from the gel	pET24a	Ligation buffer	T4 DNA ligase	Sterile water
11µl	1µl	2µl	0,5µl	5,5µl

Reaction proceeded for 2h at room temperature. As a negative control 11µl of sterile water were added except of DNA.

3.6 Transformation

Preparation of the agar plates:

8,75g of LB agar were solubilized in 250 ml of water and the solution was sterilized by autoclaving at 121°C for 15 min. Chilled solution (~ 60°C) was supplemented by 250µl of kanamycin (40mg/ml).

The host strain *E. coli* DH5α (Novagen) was transformed by a ligated vector. The procedure was carried out as follows [60,61]: 20µl of the solution after ligation were injected into 200µl of competent cells and left 30 min on ice, followed by heat shock – (42°C/90s and 2 min on ice). Cells were then incubated with 1ml of medium (without kanamycin) at 37°C for 1h. Culture was spread on the plates and incubated overnight at 37°C.

3.7 Minipreparation of the Plasmid DNA

Solutions and other material :

solution I : 25 mM Tris-HCl, 50 mM glucose, 10 mM EDTA; pH 8,0

solution II : 0,2 M NaOH, 1% (w/v) SDS – prepared before using

solution III : 3 M potassium acetate, 2 M CH_3COOH

DNA Lego kit (TopBio, CZ)

A single colony of transformed cells, freshly grown on an LB $^{KAN+}$ agar plate, was picked and inoculated into 12ml of sterile medium supplemented by kanamycin (40mg/ml). The cells were grown in a rotary incubator (Innova 4300, New Brunswick Scientific) at 37°C and 240 rpm, overnight. The culture was centrifuged (3300g, 10min, 4°C) and the cell pelet was suspended in 200µl of Solution I, 30µl of lysozyme (10mg/ml) and 7µl RNAse (10mg/ml). 400µl of Solution II were added into the suspension. The whole suspension was slightly stirred and left for 6 min on ice. The same procedure was repeated with 300µl of Solution III. The suspension was centrifuged (16000g, 7 min, 25°C) and approximately 850µl of the supernatant were transferred into an Eppendorf tube

containing 1,2ml of binding buffer (DNA Lego kit, TopBio). 200µl of the silicon microparticles were injected into the minicolumn and they were subsequently divested of the solution. Then the DNA solution was added and also divested of the solution. The sililicon microparticles with binded DNA were twice washed with DNA washing buffer. The attached DNA was eluted by 200µl of sterile water and centrifuged (16000g, 1 min). The DNA solution was supplemented by another 100µl of sterile water, 33µl of 3M sodium acetate and 666µl of 96% ethanol. DNA was precipitated at -70°C for 1h. After precipitation, the sample was centrifuged (16000g, 20 min, 25°C) and the pelet washed by 200µl of 70% ethanol and dissolved in 20µl of sterile water. The quality and quantity of DNA were verified by horizontal agar gel electrophoresis (chapter IV.3.3).

3.8 Maxipreparation of the Plasmid DNA

Solutions :

solution I : 25 mM Tris-HCl, 50 mM glucose, 10 mM EDTA; pH 8,0

solution II : 0,2 M NaOH, 1% (w/v) SDS – prepared before using

solution III : 3 M potassium acetate, 2 M CH_3COOH

TE buffer : 10 mM Tris-HCl, 1 mM EDTA; pH 8,0

A single colony of transformed cells (200µl of DH5α competent cells were transformed by 2µl of DNA from minipreparation, chapter IV.3.7) was picked and inoculated into 500ml of sterile LB medium supplemented with kanamycin (40mg/ml). The cells were grown in a rotary incubator at 37°C, 240 rpm, overnight. The culture was centrifuged (15300g, 10 min, 4°C) and the supernatant was discarded. The cell pelet was suspended in 20ml of Solution I, 1 ml of lysozyme (25mg/ml) was injected into the solution and the whole suspension was stirred for 20 min at room temperature. The suspension was then supplemented by 40 ml of Solution II and left for 10 min at room temperature. 30 ml of Solution III were added, the suspension was properly stirred and left for 10 min on ice. The suspension was centrifuged (15300g, 10 min, 4°C). The supernatant was filtered through the gauze into new cuvette, then it was supplemented with 60 ml of isopropanol, left for 10 min at room temperature and centrifuged (15300g, 10 min, 25°C). The supernatant was properly discarded and the pelet was suspended in 4 ml of TE buffer.

1,5 ml of 10M LiCl and 300µl of 1M Tris-HCl (pH 8,0) were added into the solution and the whole solution was left for 40 min on ice. The solution was centrifuged (3500g, 10 min, 4°C) and the supernatant was supplemented by 6 ml of isopropanol and left for 10 min at room temperature. After centrifugation (3500g, 10 min, 25°C), the pelet was suspended in 0,5 ml of buffer TE supplemented with 10µl of RNAse (10mg/ml) and incubated at 37°C for 1h. Futher, 0,5 ml of 13% PEG 8000 (w/v) in 1,6M NaCl was added and the whole suspension was properly stirred, centrifuged (16000g, 5 min, 25°C) and the pelet suspended in 0,5 ml of buffer TE. DNA solution was purified by the phenol/chloroform extraction as follows: 1x with the same volume of phenol, 2x with the same volume of phenol/chloroform (1:1) and 2x with the same volume of chloroform (the emulsion was always shaked, centrifuged 16000g, 5 min (only 1 min in the case of chloroform extraction) and the upper phase was taken). After the last extraction, 3M sodium acetate (1/10 of the whole volume) and 96% ethanol (2,5-fold of the total volume) were added, the sample was shaked properly and left precipitated for 15 min at room temperature. After centrifugation (16000g, 10 min, 25°C), the pelet was washed with 200µl of 70% ethanol and left for 3 min to dry. DNA was suspended in 300µl of sterile water and stored at -20°C. The quality and quantity of DNA were verified by horizontal agar electrophoresis (chapter IV.3.3).

3.9 DNA Sequencing

The DNA coding region for HIV PR was sequenced after subcloning into the bacterial plasmid pET24a using the BigDye Terminator Cycle Sequencing Ready Reaction Kit (Perkin-Elmer).

Sequencing mixture:

Compound	Volume
Sequencing buffer	4µl
Sterile water	7µl
Sequencing mix *	4µl
primer : T7 promotor (10pmol/µl) or T7 terminator (10pmol/µl)	1µl
DNA template (after miniprep)	4µl

* Sequencing mix contains: buffer Tris-HCl (pH 9,5), MgCl2, *AmpliTaq* DNA polymerase, deoxyribonucleotidtriphosphates (dATP, dCTP, dGTP, dTTP), dideoxyribonucleotidtriphosphates (ddATP, ddCTP, ddGTP, ddTTP)

The amplification was carried out under following conditions:

1) 95°C/30s
2) (95°C/10s – 50°C/5s – 60°C/4min) 25 cycles

The DNA solution was supplemented by 2µl of 3M sodium acetate and 50µl of 96% ethanol. DNA was precipitated for 15 min on ice and subsequently centrifuged (16000g, 16 min, 25°C). The pelet was washed by 200µl of 70% ethanol and dried at 90°C for 2 min. Then 20µl of TSR buffer were added, the solution was heated at 95°C for 5 min and left for 5 min on ice. The sequencing reaction products were analysed on an ABI Prism 310 DNA sequencer (Perkin-Elmer) by Petr Pajer (IMG AS CR).

3.10 Construction of HIV-1 PR Mutants by Site-Directed Mutagenesis

Mutagenesis reactions were performed using the instructions from the QuikChange® Site-Directed Mutagenesis Kit [62]. The seven proteases mutants were constructed on the basis of the patient-derived protease (K4) containing mutations: L10I, L24I, L33F, M46L, I54V, L63P, A71V, V82A and I84V. The primer pairs used to construct each protease mutations were as follows: K20R, 5′- GGGGGGCAGCTAAGGGAAGCTCTAATAG- 3′ and 5′- CTATTAGAGCTTCCCTTAGCTGCCCCCC- 3′; F53L, 5′- GGGGGAATTGGAGGTTTAGTCAAAGTAAGAC- 3′ and 5′- GTCTACTTTGGTGAC TAAACTCCAATCCCC- 3′; L90M, 5′- GGAAGAAATCTGATGACTCAAATTGGC- 3′ and 5′- GCCAATTTGAGTCATCAGATTTCTTCC- 3′. In all three cases, just a single point mutation was required.

PCR mixture:

Compound	Volume
Pfu DNA polymerase buffer (10x)	5 µl
Sterile HPLC water	40 µl
10mM dNTP	1 µl
Pfu DNA polymerase	1 µl
Forward primer (10µM)	1 µl
Reverse primer (10µM)	1 µl
DNA template-K4 after minipreparation	1 µl
Mixture volume	50 µl

Chemicals and enzymes for PCR reaction were provided by TopBio (CZ) and Promega (CZ). PCR reactions were performed in a thermocycler GeneAmp PCR System 2400 (Perkin-Elmer) under following conditions:

1.) 95°C/30s

2.) (95°C/30s - 55°C/1min - 68°C/5min) 12 cycles

3.) 72°C/8min - 4°C

Primers were synthesized by Jena Bioscience (Germany). Amplification was checked by electrophoresis of 5 µl of the product on a 1,3% agaroce gel (chapter IV.3.3).

3.11 DpnI Digestion of the Amplification Products

1µl of the *DpnI* restriction enzyme (10U/µl) was added directly to each amplification reaction. The mixture was gently mixed by pippeting the solution up and down several times. The reaction mixture was immediately incubated at 37°C for 1h to digest the parental (i.e., the nonmutated) dsDNA [62].

4. Protein Expression and Isolation

Nine enzymes have been employed in the lopinavir-resistance phenotypic study: two patient-derived HIV-1 proteases (K1, K4) and seven mutated proteases (K4 ^{K20R}, K4 ^{F53L}, K4 ^{L90M}, K4 $^{K20R, F53L}$, K4 $^{K20R, L90M}$, K4 $^{F53L, L90M}$, K4 $^{K20R, F53L, L90M}$) based on a highly resistant specimen from a patient (K4). All HIV-1 PR coding regions were ligated into a pET24a vector (chapter IV.3.5), amplified (chapter IV.3.1 and IV.3.10) and each inserted DNA sequence was verified by DNA sequencing (chapter 3.9).

4.1 HIV-1 PR Expression in E. coli

200µl of *E.coli* BL21(DE3)RIL strain (Novagen) were transformed by 2µl of expression vector pET24a containing the relevant HIV-1 PR coding sequence. The transformation with recombinant plasmids was carried out as described in chapter IV.3.6. Proteases were thus overexpressed by using of T7 promoter/T7 RNA polymerase transcription/translation system [63]. The *E.coli* BL21(DE3)RIL competent cells contain chromosomally integrated copies of *lacUV5* controlled T7 RNA polymerase and it is therefore inducible by IPTG. This expression system has an extremely low basal level expression due to the double repression by *Lac* repressor of both T7 promoter and the T7 RNA polymerase.

The expression of all nine HIV-1 proteases was performed as follows. Colonies freshly grown on an LB^{KAN+} (40µg/ml) agar plate were suspended in 12 ml of sterile LB-medium supplemented with kanamycin (40µg/ml). 1 ml of the culture was inoculated into 0,5 l of sterile LB-medium supplemented with kanamycin (40µg/ml). Finally 3 liters of the cell culture were grown in a rotary incubator (Innova 4300, New Brunswick Scientific) at 37°C and 220 rpm. When the OD_{595} reached approximately 0,8, the expression was induced by the addition of IPTG to a final concentration of 0,75 mM. After 3h the bacterial cells were peleted by centrifugation (6000g, 10min, 4°C). The cell pelet was weighted (=wet biomass) and stored at -70°C for further use. Before and 3h after the induction, the sample for SDS-PAGE analysis was taken. Cell suspension was centrifugated (16000g, 3 min) and the pelet was suspended in 100µl of PBS buffer.

4.2 Isolation of Inclusion Bodies

Buffers:

buffer A : 50 mM Tris-HCl, 50 mM NaCl, 1 mM EDTA; pH 8,0

buffer SA : 50 mM Tris-HCl, 1M NaCl, 1 mM EDTA; pH 8,0

buffer TA : 50 mM Tris-HCl, 1% (v/v) Triton X100, 1 mM EDTA; pH 8,0

The cell pelet was suspended in buffer A (10ml/1g wet biomass), supplemented with the serine protease inhibitor- PMSF (0,05mg/1g wet biomass). The suspension was three-times freeze-thawed to assist mechanical disruption of the cell walls. Subsequently, lysozyme was added (3,5mg/1g wet biomass) and the mixture was stirred for 30 min at room temperature. To assist lysis, 1% (w/v) sodium deoxycholate was added (0,5mg/1g wet biomass) and the mixture was left stirring for 20 min at room temperature. The resulting viscous suspension was sonicated 3x1min on ice (Soniprep 150) and then centrifuged (15300g, 10min, 4°C). The pellet was weighted and resuspended in buffer SA (10ml/1g wet pellet) followed by sonication and then centrifuged in the same way as previously. The washing, sonication and centrifugation steps were repeated also with buffer TA and again with buffer A. Finally, the suspension was centrifuged and the pelet of purified inclusion bodies was stored at -20°C for further use. The course of the procedure was monitored by SDS electrophoresis (chapter IV.6.1)

4.3 HIV-1 PR Renaturation

Buffers:

buffer C: 0,2 M Tris-HCl, 0,1 M Na_2HPO_4, 0,5% 2-mercaptoethanol, 0,02 M EDTA; pH 7,0

dialysis buffer : 50 mM Tris-HCl, 4 mM EDTA, 10% glycerol, 0,1% 2-mercaptoethanol; pH 7,5

Isolated and purified inclusion bodies (~1g) contain denaturated HIV-1 protease. The pellet was solubilized in 67% (w/v) acetic acid, refolded by dilution into 25-fold

excess of water and left stirred at 4°C for 15min. The whole solution was dialysed 3h at 4°C against 3 liters of water and then against dialysis buffer at 4°C overnight. Total time of dialysis was about 16h. The solution was dialysed in dialysis tubes (Spectrapore) of molecular weight cutoff 6-8 kDa. The dialysate was centrifuged (15300g, 30min, 4°C) and supernatant was further purified by cation exchange chromatography using MonoS FPLC (Pharmacia). The pellet of unsolubilised inclusion bodies was stored at -20°C for second round of refolding. The course of dialysis was monitored by SDS electrophoresis (chapter IV.6.1)

5. Purification of HIV-1 PR

Buffers:

buffer A (pH 5,8) : 50 mM MES, 10% glycerol, 1 mM EDTA, 0,05% 2-mercaptoethanol

buffer B (pH 6,7) : 50 mM MES, 10% glycerol, 1 mM EDTA, 0,05% 2-mercaptoethanol, 2 M NaCl

Dialysate containing HIV-1 protease was centrifuged (15300g, 20min, 4°C) and supernatant was filtrated through the filter unit 0,22 μm (Millipore) before it was purified on MonoS HR5/5 column (Pharmacia) by cation exchange FPLC (ÄKTA explorer, Amersham Pharmacia Biotech). The column was washed with 20ml of buffer A followed by 10ml of buffer B. After sample application, column was washed again with 10ml of buffer A. HIV protease was eluted by linear gradient from 0 to 40% buffer B. Chromatography was monitored by on-line measurement of absorbance at 280nm. The peak fractions were screened for protein concentrations (chapter IV.6.2), protease activity (chapter IV.7.2) and analysed by SDS electrophoresis (chapter IV.6.1). The fractions containing purified and active HIV protease were stored at -20°C.

6. Protein analysis

6.1 SDS-Polyacrylamid Gel Electrophoresis

Buffers:

Sample buffer (6x) : 3,5 ml 1M Tris pH 6,8; 3 ml glycerol; 1 g SDS; 0,93 g DTT or 600µl 2-mercaptoethanol; 1,2 mg bromfenol blue; water to 10ml.

Electrode buffer : 25 mM Tris, 250 mM glycin, 0,1% SDS

Expression and isolation of inclusion bodies, refolding and purification procedures were monitored by discontinuous SDS-polyacrylamide gel electrophoresis (chapter IV.6.1). Gels were prepared from a stock solution of 44% acrylamide (42,8g acrylamid, 1,2g N,N′-methylenbisacrylamid, per 100 ml water). The composition of 5% stacking and 18% resolving gels were as follows:

5% gel: 1,25ml 1,5M Tris-HCl pH 6,8; 570µl 44% acrylamide; 0,5ml 50% glycerol; 35µl 0,2M EDTA; 50µl 10%(w/v) SDS; 10µl TEMED; 100µl 10%(w/v) APS ; 2,6ml water

18% gel: 2,5ml 1,5M Tris-HCl pH 8,8; 4,09ml 44% acrylamide; 1ml 50% glycerol; 70µl 0,2M EDTA; 100µl 10%(w/v) SDS; 10µl TEMED; 90µl 10%(w/v) APS; 2,21ml water

The samples were denaturated by boiling for 5min in the sample buffer. Electrophoresis was carried out in a vertical electrophoresis apparatus (Sigma-Aldrich) ang gels were run in a constant voltage of 150 volts for 1h. The separated proteins were silver stained according to following procedure:

Step	Buffers	Time
1.	12% (v/v) acetic acid, 50% (v/v) methanol, 0,02% (v/v) formaldehyd	30min
2.	50% (v/v) methanol	3x15min
3.	$Na_2S_2O_3.5H_2O$ (0,2 g/l)	1min
4.	water	3x20s
5.	$AgNO_3$ (2g/l); 0,02% (v/v) formaldehyd	20min
6.	water	3x20s
7.	Na_2CO_3 (60g/l); $Na_2S_2O_3.5H_2O$ (4mg g/l); 0,02% (v/v) formaldehyd	developement

8.	water	3x20s
9.	12% (v/v) acetic acid, 50% (v/v) methanol	10min
10.	10% (v/v) acetic acid	overnight

Stained gels were then equilibrated in 25% (v/v) ethanol and 3% (v/v) glycerol for about 30 min and either dried between two celophane sheets at room temperature for at least 24h or the gels were scaned.

6.2 Determination of Protein Concentration

Protein concentration was determined according to Bradford [64] by measuring absorbance at 595 nm of a complex of proteins with Coomassie Brilliant Blue-G 250. Bovine serum albumin was used as a standard.

7. Kinetic Measurements

All kinetic measurements were performed using a standard spectrophotometric assay with the chromogenic peptide substrate KARVNle*NphEANle-NH_2 [65]. The peptide is derived from CA-p2 cleavage site in the HIV Gag and Gag-Pol polyprotein and it contains p-nitrophenylalanin chromophore at position P1′. Upon the substrate cleavage of the scissile bond (denoted by asterics), the decrease in absorbance at 305 nm was monitored.
The inhibition constants K_i were determined for the clinically used inhibitors lopinavir, amprenavir, saquinavir, ritonavir, indinavir and pseudopeptide inhibitor QF34 designed in the laboratory of J. Konvalinka [45].

7.1 Experimental Conditions

All measurements were performed at 37°C in buffer containing 0,1M sodium acetate (pH 4,7), 4mM EDTA and 0,3M NaCl. The course of the reaction was monitored by measuring the decrease in absorbance in 1 ml of the reaction mixture in 1 cm cuvettes at 305 nm, using an UV-VIS spectrophotometer UNICAM Heλios Alpha (CZ).

7.2 Determination of Parameters in Michaelis-Menten Equation

Michaelis-Menten constant K_m and the catalytic efficiency of the enzyme k_{cat} were determined from measurements of the initial reaction rates (v_o) in the presence of varying substrate concentrations. The initial reaction rates were measured at least at 10 different substrate concentrations ranging usually from 10 - 350μM. The data were analysed using the program Grafit 5.0.4 (Erithacus Software Limited) [66], which offers the classical Michaelis-Menten equation:

$$v_o = \frac{V_{lim} \cdot [S]}{K_m + [S]}$$

where v_o is the initial reaction rate, K_m is Michaelis-Menten constant, [S] is concentration of the substrate and V_{lim} is limit reaction rate.

The value of k_{cat} was calculated from the following equation:

$$k_{cat} = \frac{V_{lim} \cdot [S]}{\Delta A \cdot [E]_o}$$

Concentration of the active enzyme [E_0] was determined by titrating its active site by tight-binding inhibitor QF34 [67]. Substrate concentration was near K_m of the enzyme and the reaction was started by the addition of the constant emount of the enzyme. The change of the absorbance ΔA after total cleavage of the substrate was performed by analysing 40 min long reaction between substrate and enzyme.

7.3 Determination of Inhibition Constants

At least 10 values of the initial reaction rates were measured. Typically, 8 pmol of PR was added to 1 ml 0.1 M sodium acetate buffer, pH 4.7, 0.3 M NaCl and 4 mM EDTA, containing subtrate in concentration near Km of the enzyme and various concentrations of an inhibitor dissolved in DMSO. The final concentrations of DMSO were kept below 2.5%. The Ki′ values were calculated by the me Grafit 5.0.4 using the equation for competitive inhibition according to Williams and Morrison [68,69]:

$$(v_i/v_o)^2.\,[E] + ([E] + [I] - K_i').(v_i/v_o) - K_i' = 0,$$

where [E] is enzyme concentration, [I] is concentration of the inhibitor, $v_{i(0)}$ is initial reaction rate with (without) the presence of the inhibitor and K_i' is apparent inhibition constant.

K_i value was calculated from the equation:

$$K_i = \frac{K_i'}{1 + \frac{[S]}{K_m}}$$

The K_i > 100nM were calculated using me Enzfitter (Elsevier-Biosoft) according to Dixon equation [70]:

$$\frac{1}{v_i} = \frac{1}{V_{lim}}\left(1 + \frac{K_m}{[S]\,(1 + [I]\,/\,K_i)}\right)$$

8. Crystallization

Buffers:

Buffer A: 5mM MES, 1mM EDTA, 0,05% 2-mercaptoethanol, pH 6,0

Buffer B: 1M HEPES, pH 7,0

The HIV-1 PRs for crystallization were prepared and purified as described above and stored at -20°C. The complex was prepared by mixing the enzyme with 5-fold molar excess of lopinavir dissolved in DMSO and buffer A; and then concentrated to 7 mg/ml by ultrafiltration using Centricon-10 devices (Millipore).

For the crystallization trials the sparse matrix method was used [71] in combination with vapour diffusion technique [72]. For improving crystal quality, other optimazation and seeding techniques were used.

8.1 Vapour Diffusion Crystallization Technique

Crystals suitable for X-ray analysis were grown by the hanging drop vapor diffusion technique in 24 well Nextal plates (Nextal Technologies, Canada), at 19°C [72]. The crystallization drops had 2:1 ratio by volume of protein to reservoir solution. They were placed on a silliconized cover slide inverted over a 1 ml reservoir precipitating solution containing 1M $(NH_4)_2HPO_4$ as a precipitate and buffer B of pH 7,25. Pyramid shaped crystals grew in 3 days.

8.2 Crystal Seeding

Streak seeding technique using cat whisker as the probe [73] as well as macro- and micro- seeding techniques [74] were applied for improving crystal quality.

8.3 Crystal Mounting, Cryocooling and Storage

For diffraction measurement at temperature 100K, crystals were mounted into a nylon fiber CryoLoop (Hampton Research, USA) and soaked in the reservoir buffer solution with 30% (v/v) glycerol. Crystals were then flash-cooled to the liquid nitrogen temperature in a nitrogen gas stream (Oxford Cryosystem) on a goniometr head or they were storaged in a liquid nitrogen container for the next analysis.

8.4 Data Collection, Structure solution and Analysis

Data collection and processing as well as structure determination and analysis were done by RNDr. Jiří Brynda CSc. from The Institute of Molecular Genetics, Academy of Science of the Czech Republic, Prague.

X-ray diffraction data were collected on Mar345 image plate system using Nonius FR591 rotating anode generator and they were processed using program SCALA [75]. Structure was solved by EPMR program version 2.5 [76] using the searched structure of wild type HIV-1 protease complexed with lopinavir (PDB code 1MUI) [22]. Model of the structure was refined by REFMAC 5.1.24 [20]. Crystal parameters and data collection statistics are summarized in *Table V5,6.*

V. Results

1. Patient

In order to identify the relative contributions of individual mutations on the lopinavir-resistance phenotype, we used two proteases from an HIV-positive patient (code name CZ13), who was closely watched for the presence of resistant HIV species, and whose genotyping suggested resistance development to the protease inhibitor lopinavir.

We monitored the values of viral load and CD4+ T cells of patient CZ13 and the coresponding therapy with PR inhibitors (*Figure 20*). Two samples were taken from the patient in the time points indicated by red arrows. From the first sample (K1) taken in the 21st month after the start of indinavir therapy, PR species involving mutations at positions 46, 63 and 82 was isolated. After 65 months of the PI treatment and 24 months after the start of Kaletra treatment, the second sample was taken. The corresponding PR species (K4) involves all but three mutations from the lopinavir mutation score (L10I, L24I, L33F, M46L, I54V, L63P, A71V, V82A and I84V). The only exception is mutation L33F, but it

A)

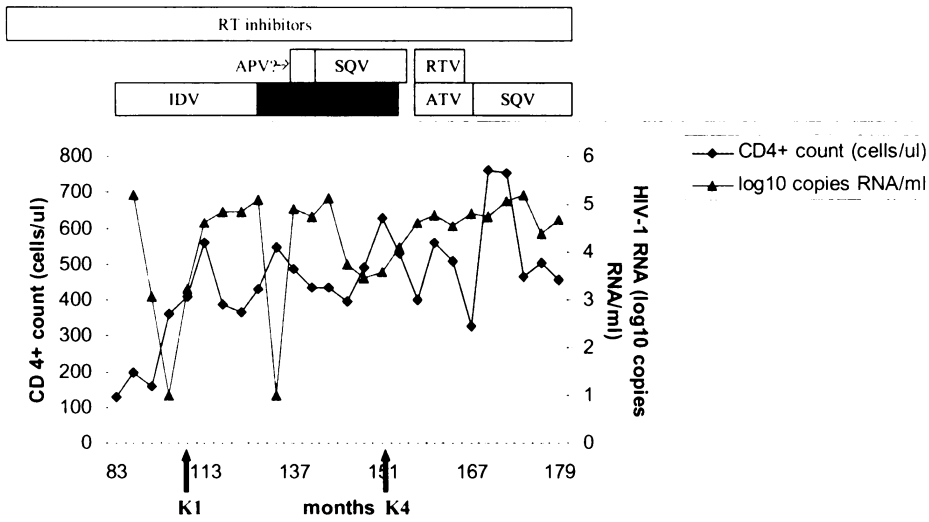

B)

Sample	Mutations in the Protease Coding Region
K1	M46L, L63P, V82A
K4	L10I, L24I, L33F, M46L, I54V, L63P, A71V, V82A, I84V

Figure 20: **Treatment of patient CZ13.** (A)Virologic (log_{10} copies of HIV-1 RNA/ml of plasma) and immunologic ($CD4^+$ cell count) response in correlation of PI-therapy of patient CZ13. Two samples were taken from the patient in the time points indicated by red arrows. (B) K1 and K4 patient-derived proteases and their list of amino acid mutations compared to consensus B sequence. Graf starts at 83th month of the treatment.

seems likely that this mutation contributes to LPV resistance as well. Only the mutations K20R, F53L and L90M in the K4 PR coding region of patient CZ13 are missing to complete lopinavir mutation score. In order to identify the mutations critical for the LPV resistance, we used this sequence as a framework for engineering a panel of mutants that involve all amino acid substitutions from the lopinavir mutation score (i.e., adding mutations K20R, F53L, L90M alone or in combination (see *Figure 21*)).

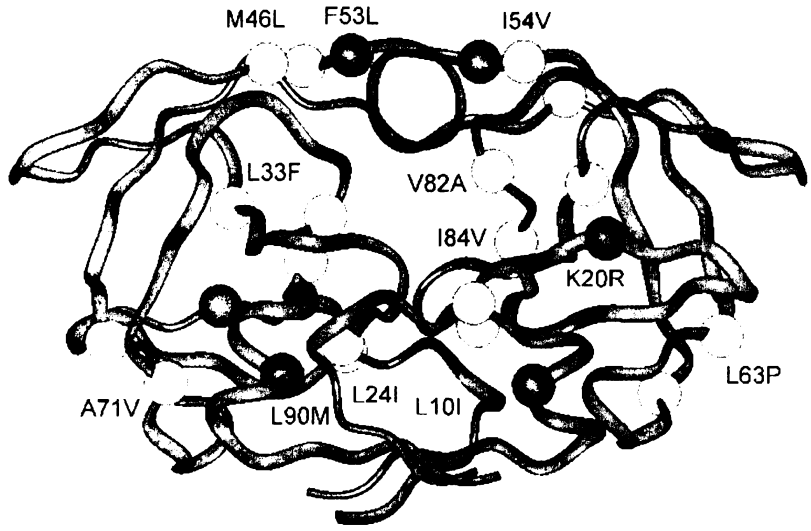

Figure 21: **Model of K4 protease used as a framework for introducing the remaining mutations to complete lopinavir mutation score**. Residue changes in K4 patient-derived protease are marked by yellow spheres. Mutations ingeneered onto K4 variant backround are shown in red. The figure was created by Martin Lepšík (IOCB AS CR).

2. Generation of Recombinant HIV-1 Proteases

Both patient-derived HIV-1 protease coding regions were amplified by PCR method using two primers with *NdeI* and *EcoRI* cleavage sites. PCR products were then cleaved by *NdeI* and *EcoRI* restriction endonucleases and reaction mixtures were separated by horizontal agar gel electrophoresis. DNAs of HIV-1 PRs were subsequently isolated from the gel and the identity of the product was verified again by agar gel electrophoresis. HIV-1 PR coding regions were then ligated into the expression vector pET24a, cleaved by *NdeI* and *EcoRI*.

2.1 Cloning of HIV-PR Mutants by Site-Directed Mutagenesis

K4 patient-derived HIV-1 PR was used as a framework for construction of seven additional proteases to fulfill "lopinavir mutation score" and to identify the mutations critical for the viral resistance to this protease inhibitor. The panel of all proteases prepared within this study is shown in *Table 1.*

Variants	Mutations
K1	M46L, L63P, V82A
K4	L10I, L24I, L33F, M46L, I54V, L63P, A71V, V82A, I84V
$K4^{K20R, F53L, L90M}$	K4 + K20R, F53L, L90M
$K4^{L90M}$	K4 + L90M
$K4^{K20R}$	K4 + K20R
$K4^{F53L}$	K4 + F53L
$K4^{K20R, F53L}$	K4 + K20R, F53L
$K4^{F53L, L90M}$	K4 + F53L, L90M
$K4^{K20R, L90M}$	K4 + K20R, L90M

Table 1: **Variants and residue changes.** K1 and K4 indicate patient-derived HIV-1 PRs (yellow backround), whereas K4 plus superscripts marks engineered PRs; relevant mutations are summarized in the right column.

Mutagenesis reactions were performed as described in chapter IV.3.10. The PCR reaction mixtures were further incubated with *DpnI* restriction enzyme to digest the parental (i.e., the nonmutated) dsDNA. The PCR products were checked up by horizontal agar gel electrophoresis before they were used for transformation and plasmid DNA minipreparation. Finally, all DNA were verified by sequencing. As an example, the result of mutagenesis reaction where L90M substitution was introduced into the K4 protease coding region is shown in *Figure 22.*

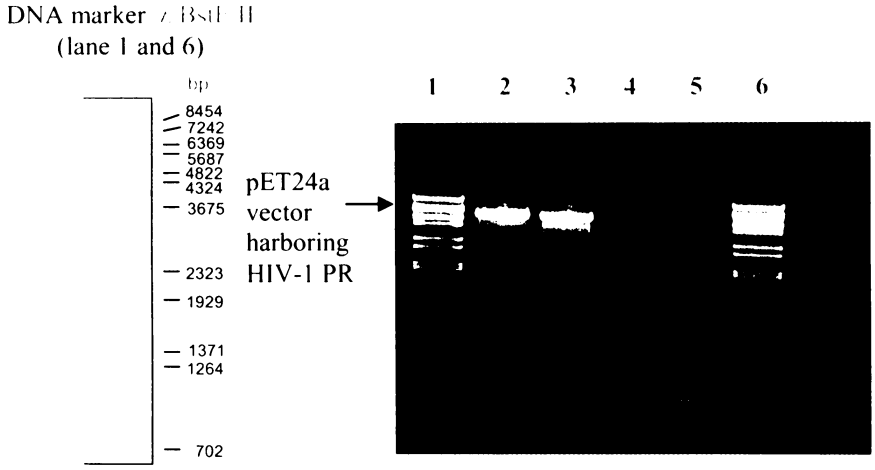

Figure 22: **DNA mutagenesis.** Lane 2, lane 3, pET24a vectors harboring K4 ^{L90M} protease coding region (two different concentrations of template K4 DNA were used for mutagenesis reactions). First negative control in lane 4 (without DNA) and second in lane 5 (same PCR mixture but without *Pfu* polymerase and no digestion with *DpnI* occured). 1,3% agarose.

3. Proteins Expression and Isolation

3.1 Expression of HIV-1 PRs

Nine HIV-1 PRs, summarized in *Table 1*, from T7 promotor-driven expression plasmid (pET24a) were expressed in *E. coli* BL21(DE3)RIL strain. The expressions were induced with IPTG (see *Figure 23*). Transformed bacteria produced within a short period of time large amounts of enzyme, which accumulates in the cytoplasm in the form of inactive insoluble aggregates, so-called inclusion bodies. After 3 hours of induction, cells were harvested. Typical yields for 1,5 liters of bacterial culture were about 5g of wet bacterial biomass.

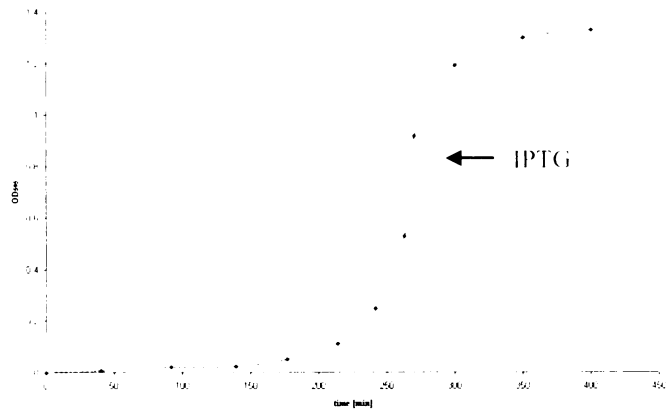

Figure 23: **Typical growth curve of *E.coli* BL21(DE3)RIL bearing HIV-1 PR expression plasmid.** Induction of IPTG is marked.

Inclusion bodies were isolated by standard procedure, described in detail in Materials and Methods. *Figure 24* shows the SDS-PAGE gel monitoring the purification process of inclusion bodies. Moreover, lane 2 and 3 represent cell culture before and after the induction, respectively. During the washing steps, some contaminating bacterial proteins are removed (lane 4-6) and inclusion bodies contain relatively large amount of HIV-1 PR (lane 8). Yields from 1,5 liters of bacterial culture were about 0.5g of partially purified inclusion bodies.

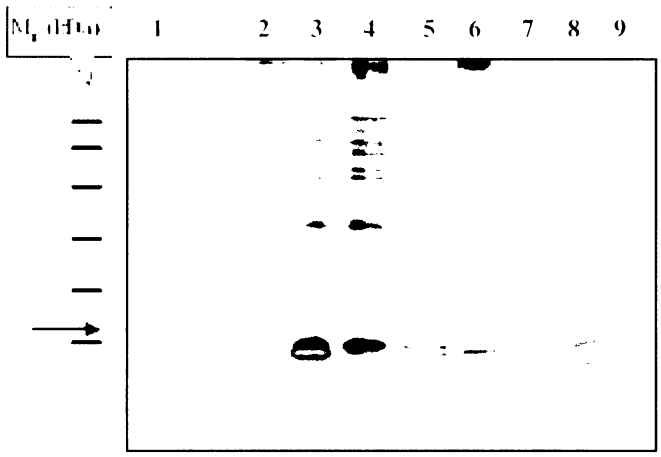

Lane 1	Molecular weight marker
Lane 2	Cell culture before induction
Lane 3	Cell cul. after induction
Lane 4	Washing step 1
Lane 5	Washing step 2
Lane 6	Washing step 3
Lane 7	Supernatant from the last washing step
Lane 8	Inclusion bodies
Lane 9	HIV-1 PR standard

Figure 24: **Example of the isolation of inclusion bodies** monitored by 18% SDS-PAGE gel under reducing conditions stained by silver staining.

Inclusion bodies contain HIV-1 PR in reduced and denaturated form. To obtain functional enzyme, solubilization and refolding procedures are required. These methods are described in Materials and Methods.

3.2 Purification of HIV-1 PRs

Purification procedure comprises only one step represented by cation exchange FPLC chromatography using MonoS HR5/5 column and yields about 5 mg of purified HIV-1 protease per 1 liter of bacterial culture. Typical course of purification of one of the recombinant protease is ilustrated in *Figure 25* and *26* with chromatographs and SDS-PAGE analysis of protein samples, respectively.

After refolding the protein solution was applied to cation exchange column. At pH 5,8; HIV-1 protease is bound to the MonoS HR5/5 column and afterwards it is eluted by gradient of 2M NaCl at pH 6,3. The main fractions are usually obtained by elution with 1,6% (w/v) NaCl (20% of buffer B).

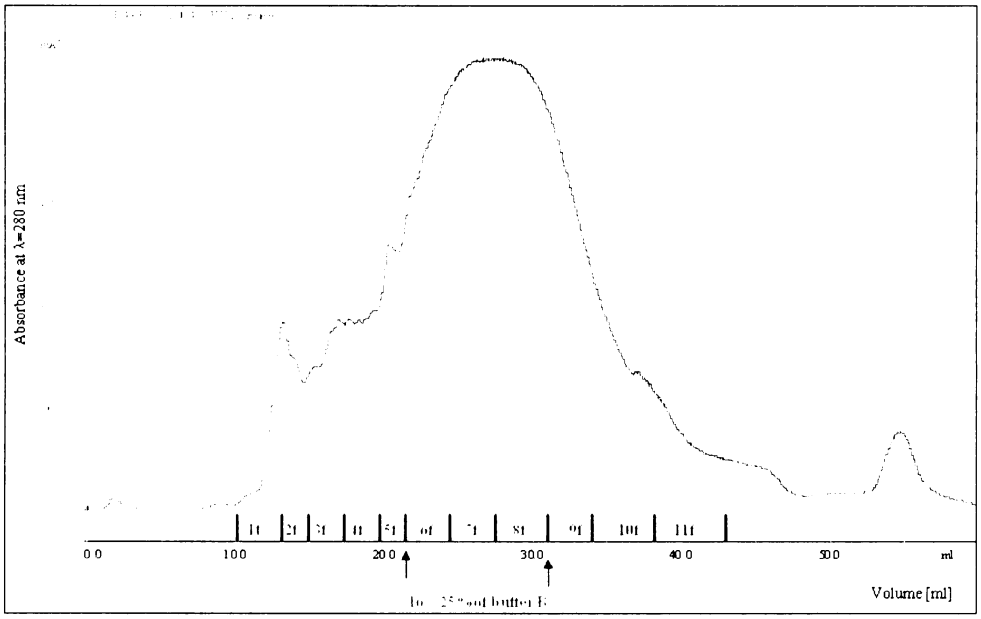

Figure 25: **Purification procedure of K4 HIV-1 PR on MonoS HR5/5 column by cation exchange FPLC.** Fractions are marked in red. Gradient of buffer B (2M NaCl) is marked by blue arrows and only for main fractions region.

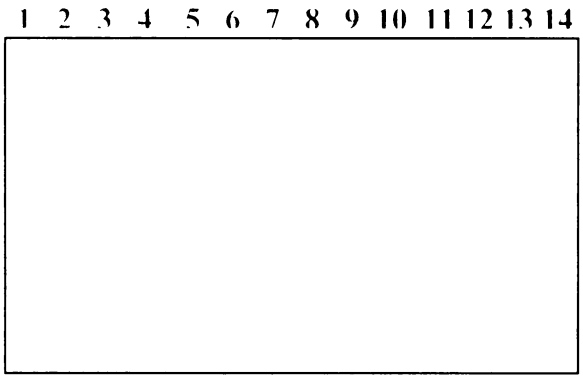

Lane 1	HIV-1 PR standard
Lane 2	Molecular weight marker
Lane 3	Supernatant before dialysis
Lane 4	Supernatant after dialysis
Lane 5	Fraction 2f of FPLC purification
Lane 6	Fraction 3f of FPLC p.
Lane 7	Fraction 4f of FPLC p.
Lane 8	Fraction 5f of FPLC p.
Lane 9	Fraction 6f of FPLC p.
Lane 10	Fraction 7f of FPLC p.
Lane 11	Fraction 8f of FPLC p.
Lane 12	Fraction 9f of FPLC p.
Lane 13	Fraction 10f of FPLC p.
Lane 14	Fraction 11f of FPLC p.

Figure 26: **The course of purification procedure monitored by reduced silver stained 18% SDS-PAGE.**

The peak fractions were screened for protein concentration and protease activity. For better evaluation of the purification process, we determined the "relative activity unit" as the activity which is responsible for the decrease in absorbance of 10^{-4} $AU.s^{-1}$ of a

chromogenic substrate cleaved by a PR preparation (measured at standard conditions, 17 μM substrate, 37°C, pH 4,7). Data from the purification procedure of K4 HIV-1 PR as a representative example are summarized in *Table 2*. In this particular case, the yield of the purification procedure was about 93%. Finally, about 10 mg of active enzyme were obtained.

Purification Table of K4 Protease							
Fraction	Volume [ml]	Activity [AU/s/μl]	Relative Activity [ru]	Yield [%]	Protein Concentration [μg/ml]	Specific Activity [ru/μg]	Purification Ratio
supernatant after dialysis	100	6,52E-05	65200,0	100	68	9,6	1
1f	2	x	x	x	x	x	x
2f	2,7	3,96E-06	107,0	0,2	166	0,24	0,02
3f	1,3	6,04E-06	78,0	0,1	232	0,26	0,03
4f	2,9	6,94E-06	201,0	0,3	258	0,27	0,03
5f	2,1	3,39E-05	712,0	1,1	286	1,18	0,12
6f	3,2	2,29E-04	7314,0	11,2	494	4,63	0,48
7f	3,1	5,38E-04	16673,0	25,6	583	9,23	0,96
8f	2,9	6,45E-04	18717,0	28,7	587	11,00	1,15
9f	4,1	3,61E-04	14782	22,7	546	6,60	0,69
10f	2,2	9,02E-05	1985	3,0	250	3,61	0,38
11f	4,4	x	x	x	x	x	x
8f + 9f (for X-ray analysis)	6	5,90E-01	35400	54,3	501	11,80	1,20
6f + 10f (for kinetic analysis)	5,4	1,72E-04	9288	14,2	395	4,35	0,45

***Table 2:* Purification table summarizing the yields of purification procedure of K4 HIV-1 PR.** The enzyme was expressed in 3 liters of bacterial culture and 7,4 g of the cells were harvested. The pelet of isolated inclusion bodies was 0,8 g. Finally, about 10 mg of active enzyme was obtained.

3.3 The Overview of All Prepared HIV-1 PRs

In total nine recombinant HIV-1 PRs were expressed and purified mostly in sufficient amount for crystallization trials. The SDS-PAGE analysis of all the enzymes is shown in *Figure 27*.

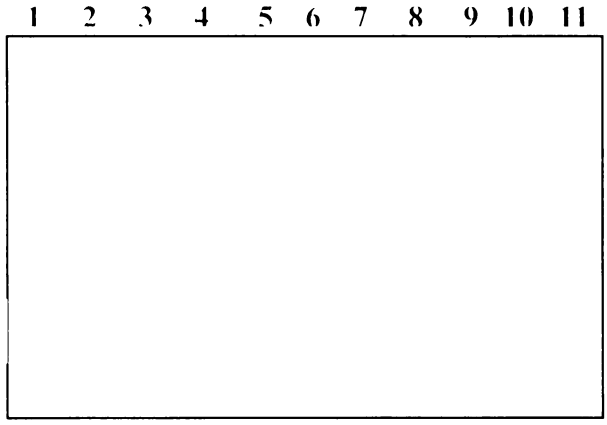

Lane 1	Molecular weight marker
Lane 2	HIV-1 PR standard
Lane 3	K1 HIV-1 PR
Lane 4	K4 HIV-1 PR
Lane 5	$K4^{K20R,\ F53L,\ I.90M}$ HIV-1 PR
Lane 6	$K4^{I.90M}$ HIV-1 PR
Lane 7	$K4^{K20R}$ HIV-1 PR
Lane 8	$K4^{F53L}$ HIV-1 PR
Lane 9	$K4^{K20R,\ F53L}$ HIV-1 PR
Lane 10	$K4^{K20R,\ I.90M}$ HIV-1 PR
Lane 11	$K4^{F53L,\ I.90M}$ HIV-1 PR

***Figure 27:* SDS-PAGE analysis of all nine recombinant enzymes prepared within this study.** Silver stained 18% SDS-PAGE, 3 ng of each particular protein.

4. Kinetic Analyses

All prepared proteases were kinetically characterized using standard spectrophotometric assay with the chromogenic peptide substrate KARVNle*NphEANle-NH_2 described in detail in Materials and Methods. We measured K_m and k_{cat} for all enzymes and their catalytic effeciency was calculated (k_{cat}/K_m). The results are summarized in *Table 3*. Kinetic characteristics for wt HIV-1 PR* were measured by J. Weber from Jan Konvalinka's lab at IOCB AS CR and they are shown as a reference.

Variants	K_m (μM)	k_{cat} (s^{-1})	k_{cat}/K_m (s^{-1} μM^{-1})
Wt*	15,1 ± 1,3	30,0 ± 1,8	1,99 ± 0,22
K1	5 ± 1	6,3 ± 0,5	1,22 ± 0,15
K4	14 ± 1	6,4 ± 0,3	0,45 ± 0,04
K4 $^{K20R, F53L, L90M}$	120 ± 13	2,7 ± 0,1	0,02 ± 0,00
K4 ^{L90M}	49 ± 3	7,3 ± 1,1	0,15 ± 0,03
K4 ^{K20R}	15 ± 1	6,6 ± 0,2	0,44 ± 0,05
K4 ^{F53L}	19 ± 2	5,5 ± 0,7	0,28 ± 0,04
K4 $^{K20R, F53L}$	29 ± 4	3,2 ± 0,3	0,11 ± 0,02
K4 $^{K20R, L90M}$	29 ± 4	2,8 ± 0,3	0,1 ± 0,02
K4 $^{F53L, L90M}$	80 ± 13	2,6 ± 0,2	0,03 ± 0,01

***Table 3*: Michaelis-Menten constants.** *Data for wt HIV-1 PR are reproduced from [78].

Catalytic efficiencies of each particular protease as compared to wild-type protease are more illustratively shown in *Figure 28*.

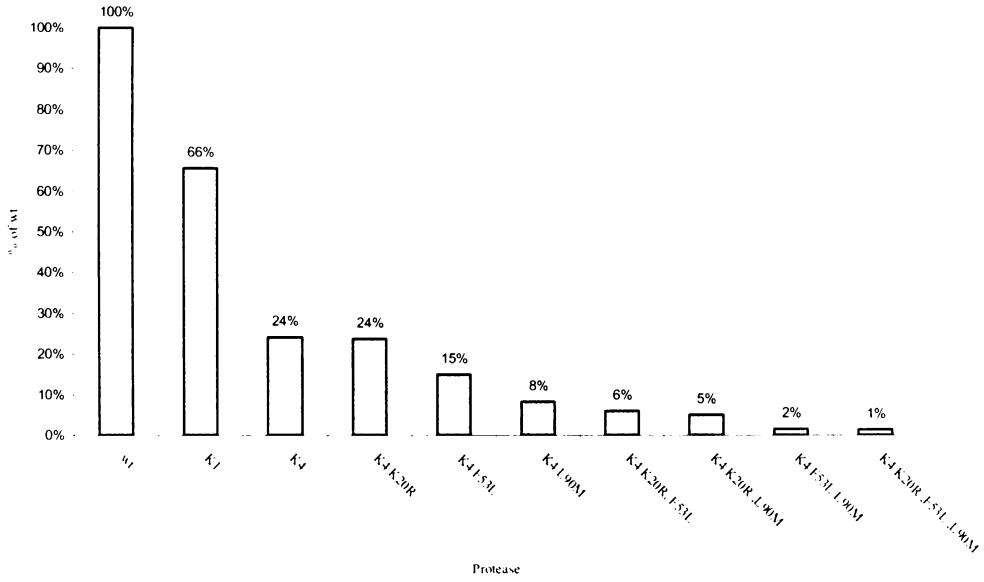

***Figure 28:* Relative catalytic effeciencies of mutated proteases compared to wt HIV-1 PR.** Values are marked out in % scale and arranged by decreasing values.

Futhermore, the inhibition constants (K_i) of all proteases were determined for the clinicaly used inhibitors lopinavir, saquinavir, ritonavir, indinavir and amprenavir and also for tight-binding inhibitor QF34, designed and tested in IOCB AS CR. These data are summarized in *Table 4.*

Variants	K_i^{LPV} (nM)	K_i^{QF34} (nM)	K_i^{APV} (nM)	K_i^{RTV} (nM)	K_i^{IDV} (nM)	K_i^{SQV} (nM)
Wt*	0,018	0,02	0,184	0,015	0,12	0,04
K1	0,32 ± 0,09	0,08 ± 0,01	0,08 ± 0,01	0,09 ±0,03	5,9 ± 0,32	0,19 ± 0,04
K4	0,44 ± 0,09	0,22 ± 0,07	4,12 ± 0,34	35 ± 3	47 ± 3	180 ± 14,82
$K4^{K20R, F53L L90M}$	9,93 ± 1,36	4,37 ± 0,67	53,6 ± 2,77	946 ± 49	1352 ± 70	2657 ± 137
$K4^{L90M}$	5,69 ± 1,13	1,36 ± 0,28	34,15 ± 0,86	980 ± 24	565 ± 14	969 ± 24
$K4^{K20R}$	0,35 ± 0,1	0,53 ± 0,03	6,76 ± 0,72	19 ± 0,88	95 ± 9	75 ± 3,6
$K4^{F53L}$	0,44 ± 0,09	1,28 ± 0,37	8,52 ± 0,36	47 ± 5	52 ± 9	356 ± 14,5
$K4^{K20R, F53L}$	0,53 ± 0,23	0,56 ± 0,23	3,24 ± 0,22	57 ± 8	74 ± 5	630 ± 42
$K4^{K20R, L90M}$	3,00 ± 0,43	10,2 ± 1,31	32,28 ± 6,16	364 ± 25	694 ± 48	1848 ± 126
$K4^{F53L, L90M}$	7,15 ± 0,72	15,4 ± 1,31	55,85 ± 5,92	421 ± 26	534 ± 45	2684 ± 227

***Table 4:* Dissociation constants (K_i) .** 8-9 pmol of PR was added to 1 ml 0.1M sodium acetate buffer, pH 4.7, 0.3M NaCl and 4 mM EDTA, containing substrate concentration near K_m of the enzyme and various concentrations of an inhibitor. The K_i values were determined according to either Williams and Morrison 's equation [68,69] or Dixon's equation [70]. *Data for wt HIV-1 PR are reproduced from [78].

The ability of individual proteases to cleave substrate in the presence of given inhibitor was compared to the wild-type values and expressed as vitality *v*, defined as $v = (K_i\ k_{cat}/K_m)_{MUT} / (K_i\ k_{cat}/K_m)_{WT}$ [79]. The higher vitality, the less sensitive given mutant is towards specific inhibitor. Vitalities for all proteases are shown in *Figure 29, panel a,b.*

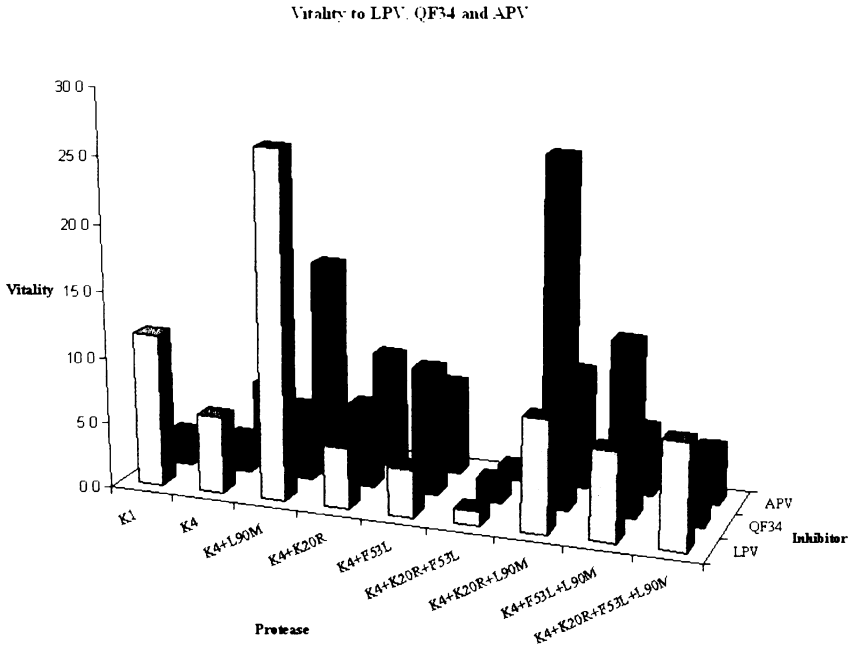

***Figure 29:* Vitality values using wild-type enzyme as a reference for all proteases with each tested inhibitor.** Vitality is defined as $v = (K_i\ k_{cat}/K_m)_{MUT} / (K_i\ k_{cat}/K_m)_{WT}$ and indicates the ability of individual proteases to cleave substrate in the presence of given inhibitor, compared to the particular wild-type values. **Panel a**: inhibitors LPV, QF34 and APV

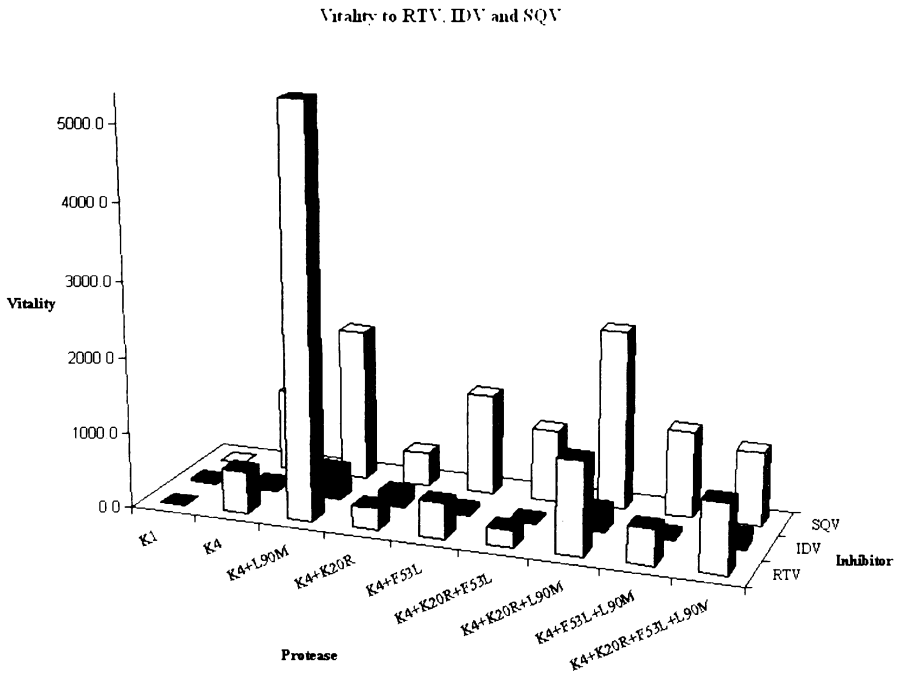

Panel b: Inhibitors RTV, IDV and SQV

5. Crystallization of HIV-1 PR in Complex with PI Lopinavir

5.1 Crystallization

Crystallization experiments were performed with highly pure and active fraction of HIV-1 PR mutant denoted $K4^{K20R,F53L}$. Regarding to previous experiences with crystallizing HIV-1 PRs in complex with various inhibitors, three specific salts as precipitants were used for initial crystallization trials – ammonium sulfate, sodium chloride and diamonium hydrogenphosphate. pH scale was also screened in first experiment. Successful condition from the initial screen (0,1M HEPES pH 7,0, 1M $(NH_4)_2HPO_4$) was selected for optimization trials. In the second screening, suitable protein concentration was found and also the pH and salt concentration were optimized. Finally, successful condition using 0,1M HEPES pH 7,25; 0,8M $(NH_4)_2HPO_4$ yielded good quality 'three dimensional' crystals, that have grown spontaneously in three days (*Figure 30*).

Figure 30: **Crystals of K4^{K20R,F53L} HIV-1 PR in complex with PI lopinavir**. Crystals (up to 0,4mm x 0,2mm x 0,2mm) were very sensitive, in few days flaws on their surface appeared.

Despite the large size of obtained crystals (up to 0,4mm x 0,2mm x 0,2mm), they were very sensitive and must have been cooled as soon as possible. 30% glycerol proved to be suitable for cryocooling and thus the crystals could be used for data collection. Selected pyramidal crystals (*Figure* 30) were used for X-ray analysis. The structure solved from data obtained from these crystals confirmed that they constist of HIV-1 PR – lopinavir complexes.

5.2 Structure determination

Crystals of K4^{K20R,F53L} HIV-1 PR – LPV complex, grown as described earlier, belong to hexagonal space group P65 with these cell dimensions: a = 61.24 Å, b = 61.24 Å, c = 98.33 Å and γ = 120°. Two complexes are present in the crystallographic asymmetric unit.

X-ray data were collected in the laboratory of J. Sedláček at IMG, AS CR, Prague by J. Brynda at cryogenic conditions using Nonius FR591 Rotating Anode Generator (source type Cu$K\alpha_{1,2}$) of wavelength 1.54179 Å. Diffraction data collection statistics are summarized in *Table 5*.

Diffraction Data Summary and Statistics of HIV-1 PR $K4^{K20R,F53L}$ – LPV complex	
Number of crystals	1
Source type	$CuK\alpha_{1,2}$
Wavelength (Å)	1.54179
Temperature (K)	100
Space group	$P6_5$
Cell parameters	
a, b, c (Å)	61.24, 61.24, 98.33
α, β, γ (°)	90, 90, 120
Complexes per asymetric unit	2
Resolution range (Å)	53.45 – 2.4
No. of observed reflections	35320
Multiplicity	4.5
Completeness (%)	99.96
Average I /σ (last resolution shell)	10.7

Table 5: **Diffraction data summary and statistics.** Done by J. Brynda in the laboratory of J. Sedláček, IMG, AS CR.

Structure was solved by molecular replacement using the searched structure of wild type HIV-1 protease complexed with lopinavir (PDB code 1MUI) [22]. The model was refined to a final R factor 22.1% and R_{free} factor 27.7%. Refinement statistics are summarized in *Table 6.*

Refinement Statistics of HIV-1 PR $K4^{K20R,F53L}$ – LPV complex	
Resolution range (Å)	53.45 – 2.4
No. of reflections	8025
R value (%)	22.066
R_{free} value (%)	27.668
R_{free} value (%) in test set size	4.6
R_{free} value in test set count	390
B for Wilson plot	48.1
Ramachadran plot	
Most favoured ragions (%)	93.7
Allowed regions (%)	6.3
Generously allowed regions (%)	0.0
Disallowed regions (%)	0.0

Table 6: **Refinement statistics for the complex of $K4^{K20R,F53L}$ HIV-1 PR and lopinavir.**

5.3 Overall Structure and the Quality of the Model

The electron density map of the structure is of high quality, there are no mainchain breaks in electron density and residues belonging to regions of the loops are well defined in the electron density map.

The comparison of the overall structure of the $K4^{K20R,F53L}$ HIV-1 PR – LPV complex (in red) versus the structure of the wild-type HIV-1 PR – LPV complex (in blue), both represented by the ribbon diagrams, is shown in *Figure 31* (the inhibitor is not shown for clarity). As expected, there are no significant structural changes which is in agreement with our kinetic observations.

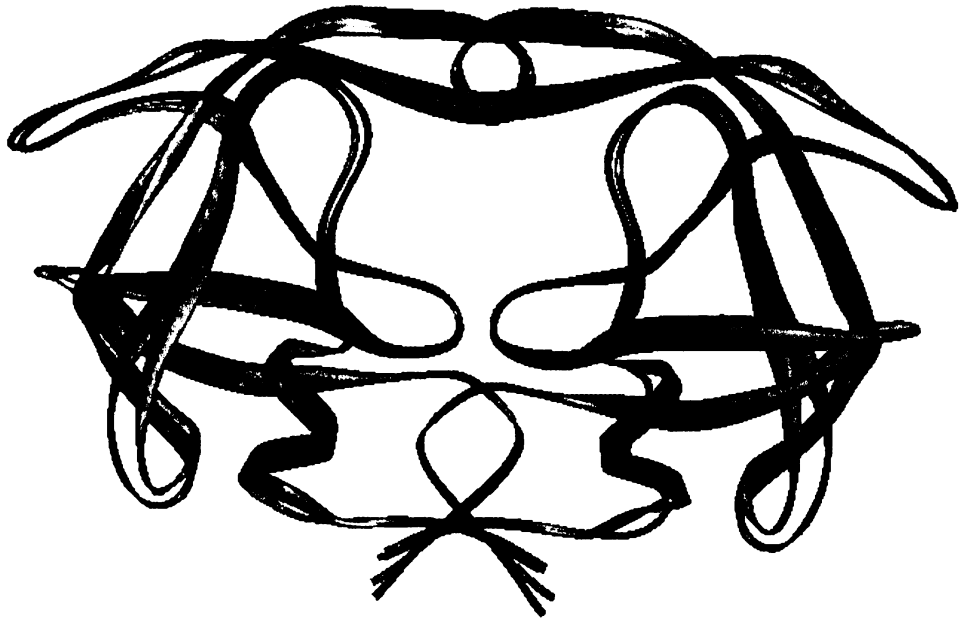

Figure 31: **The comparison of overall structures of $K4^{K20R,F53L}$ HIV-1 PR and wild-type HIV-1 PR, both in complex with lopinavir.** $K4^{K20R,F53L}$ HIV-1 PR is shown in red, while wild-type PR in blue; structures are represented by ribbons. The inhibitor is not shown. The figure was created using program ViewerLite 4.2 [80].

The torsion angles of the main chain are analyzed in a Ramachandran plot [81] produced by the program PROCHECK [82] (*Figure 32*). All residues from the model fall into favorable or allowed regions of the Ramachandran energy space.

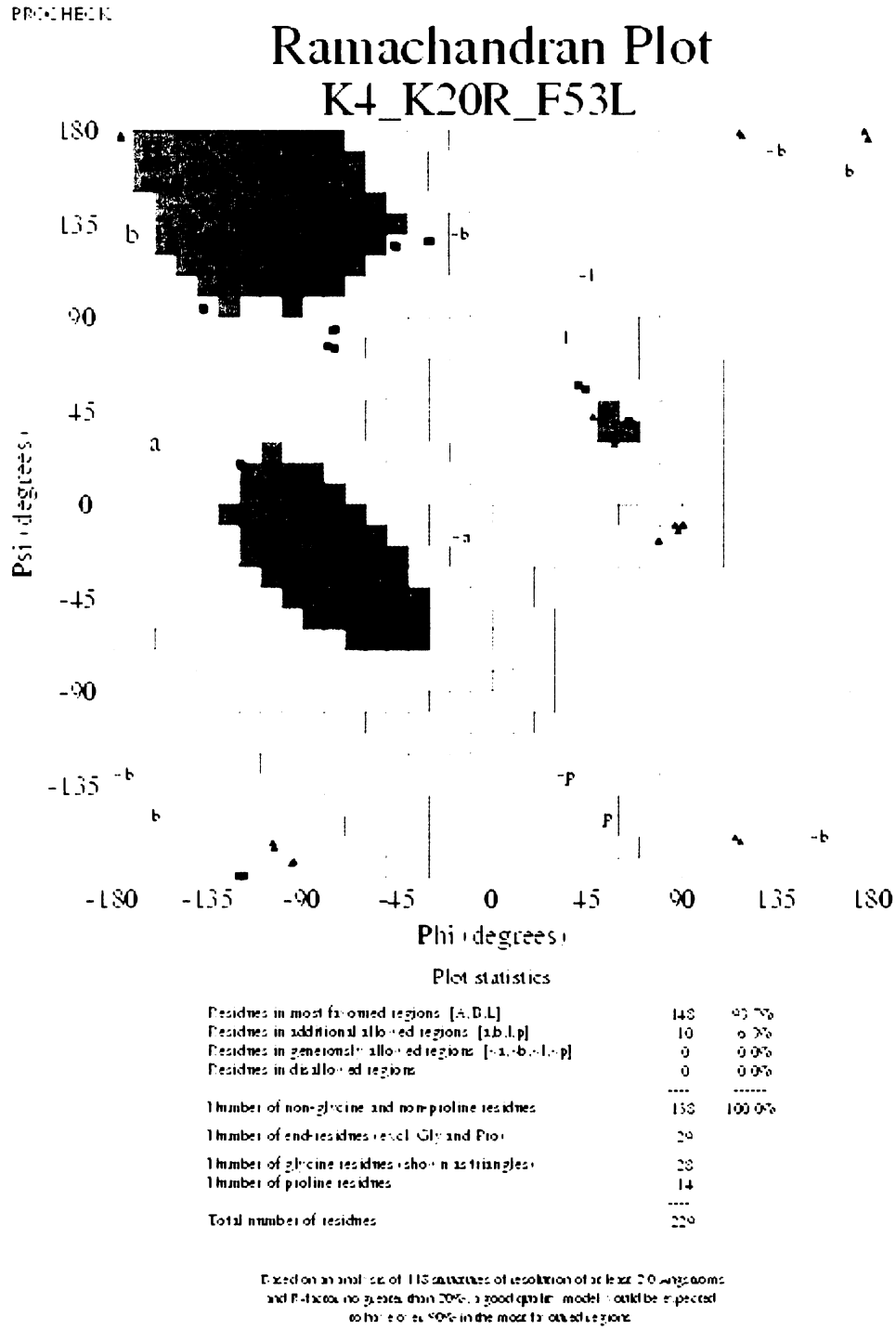

Figure 32: **Ramachandran plot of the K4^{K20R,F53L} HIV-1 PR – LPV complex structure.** The plot was produced by the program PROCHECK [82].

5.4 Conformation of Lopinavir in Complex

Similarly as in the case of wild-type HIV-1 PR in complex of lopinavir [22] we observed two clear binding modes of the inhibitor which represent a 2-fold 180° disorder in the inhibitor orientation. In another words, the inhibitor binds in two possible conformations. This 2-fold occupancy has been observed in many inhibited complexes of HIV-1 protease [83]. The overlay of these two orientations is shown in *Figure 33*, which represents the omit-electron density map of the $K4^{K20R,F53L}$ HIV-1 PR – LPV complex.

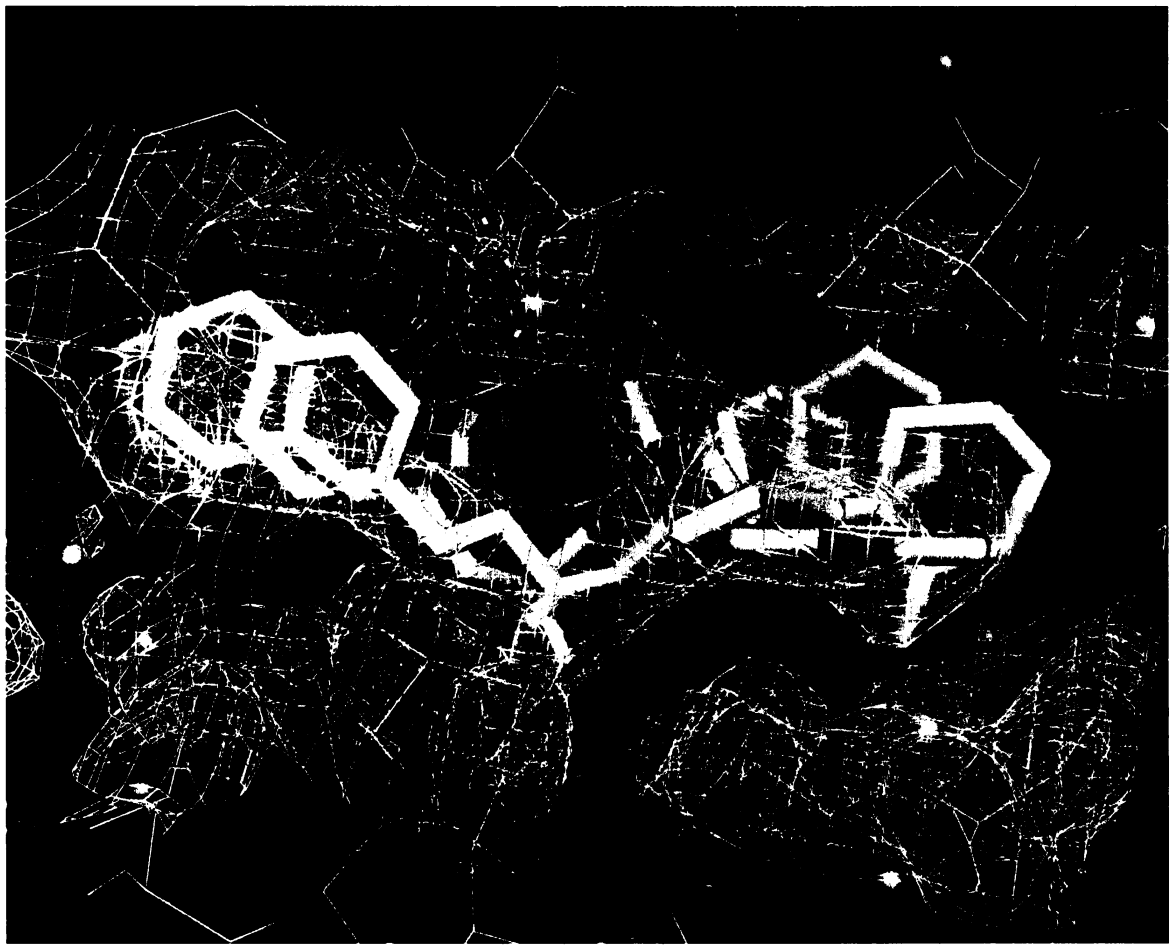

Figure 33: **The omit-electron density map of the $K4^{K20R,F53L}$ HIV-1 PR – LPV complex calculated with coefficients ($F_0 - F_C$) and phases from the refined model, contoured at 3σ level.** H-bond between LPV and Ile50 residue mediated through water molecule is marked as well as catalytic Asp25. The figure was created using program PyIMOL [21].

VI. Discussion

Lopinavir is the second-generation protease inhibitor that was rationally designed to inhibit resistant PR species and is used in combination with another PI ritonavir. The mixture of both compounds known as Kaletra is today considered an important salvage drug, which is predominantly administered when the primary therapy with PIs has failed. Even though it has been used already 5 years, its resistance profile has not been clearly defined. Mutations at 11 amino acid positions in PR coding region were identified as associated with reduced susceptibility and were termed as lopinavir mutation score. However, the precise role of each mutation should be examined by *in vitro* site-directed mutagenesis. Well defined lopinavir resistance profile may povide insights into either patients therapy or design of new inhibitors.

In patient CZ13 treated consecutively by indinavir and Kaletra, considerable number of mutations accummulated during 65 months of therapy using PIs that all belong to "lopinavir mutation score" (L10I, L24I, L33F, M46L, I54V, L63P, A71V, V82A and I84V). The only exception was mutation L33F, which does not belong to "lopinavir mutation score", but it seems likely that this mutation contributes to LPV resistance as well. Only the mutations K20R, F53L and L90M in the PR coding region of patient CZ13 were missing to complete lopinavir mutation score. We used this protease as a framework for engineering a panel of mutants that involve all amino acid substitutions from the lopinavir mutation score (i.e., adding mutations K20R, F53L, L90M alone or in combination).

We monitored the values of viral load and CD4+ T cells of patient CZ13 and the coresponding therapy with PR inhibitors. Two samples were drawn from the patient; the first sample taken in the month 21 after the start of indinavir therapy and after 65 months of the PI treatment and the second sample 24 months after the start of Kaletra treatment. The corresponding PR species were expressed in *E. coli*, purified and enzymatically characterized.

No apparent increase in resistance to lopinavir (measured *in vitro* in terms of the vitality value of the recombinant resistant PR with the panel of PR inhibitors) in this patient-derived enzymes was observed, although the therapy failed. Our aim was to find out whether the three "additional" mutations that were engineered into the framework of

K4 protease would reduce the susceptibility to lopinavir. Thereby we aimed to identify the mutations critical for the viral resistance to this protease inhibitor.

We prepared a panel of proteases by site-directed mutagenesis, that all include mutations from patient protease K4 and mutations K20R, F53L and L90M alone or in combination. These recombinant enzymes were expressed in *E. coli* and characterized enzymatically. We also crystallized and analysed 3D-structures of one protease $K4^{K20R, F53L}$ (L10I, K20R, L24I, L33F, M46L, F53L, I54V, L63P, A71V, V82A and I84V), in complex with lopinavir at resolution 2.4Å.

Kinetic Analysis. The Michaelis-Menten constants were obtained for patient-derived proteases K1 and K4 and for all recombinant proteases. The mutant protease $K4^{K20R,F53L,L90M}$, that includes all mutation from lopinavir mutation score, showed a 99% decrease in k_{cat}/K_m from that of reference wild-type protease. This decrease in catalytic efficiency was attributed to both analyzed values: a large 8-fold increase in K_m and 11-fold decrease in k_{cat} compared to wild-type. The most significant effect from all three "additional" mutations reganding K_m values revealed L90M substitution. This conclusion is clear from comparison the K_m values of $K4^{L90M}$, $K4^{K20R}$ and $K4^{F53L}$ proteases (49μM, 15μM and 19μM respectively). Almost no significant changes were observed in k_{cat} values of all engineered proteases in regard to K4 patient-derived protease. Therefore, the mutations clearly affect predominantly the substrate (inhibitor) binding rather than catalytic efficiency of the enzymes.

Inhibitor binding. The dissociation constants (K_i) were determined for the clinicaly used inhibitors lopinavir, saquinavir, ritonavir, indinavir and amprenavir and for tight-binding inhibitor QF34. In order to simply explain *in vitro* resistance to particular PI, vitality value was established as the ability of individual proteases to cleave substrate in the presence of given inhibitor compared to wild-type [79]. The higher vitality, the lower susceptibility towards PI and the higher resistance degree. Here we comment only vitalities to PI lopinavir. Three mutations in K1 patient-derived protease are responsible for moderate increase in vitality (approx. 12 times), whereas accummulation of nine mutations (K4 PR) lead to even lower increase in vitality (6 times) compared to wild-type. Almost no significant changes in susceptibility to LPV showed K20R and F53L substitutions in the

framework of K4 PR. Moreover, if both these mutations are present, they seem to have rather compensatory effect and decrese the resistance. This also explain only 8 times increase in vitality in case of $K4^{K20R,F53L,L90M}$ protease, whereas $K4^{L90M}$ protease showed very significant, 26 times increase and thus the most significant contribution to the resistance. Therefore, we calculate that L90M mutation is the critical one, contributing mostly to the resistence phenotype of all the mutations of the "lopinavir mutation score".

Structure analysis. We crystallized and analysed the 3D-structure of $K4^{K20R,F53L}$ protease in complex with PI lopinavir at resolution 2.4Å. The structural analysis revealed no significant structural changes in regard to wild-type PR which correspond with our kinetic data. Unfortunately we were not able to crystallize proteases harboring L90M mutation, that contributes most significantly to the overall resistant phenotype to PI lopinavir, mainly due to their higher K_i values towards LPV. Therefore, we can only presume in regard to other crystal structures of complexes HIV-1 PR harboring L90M mutation and PIs, that the L90M substitution has major effect on the overall structure, probably representing by open-flap conformation. The final answer could be provided by molecular dynamics study of the mutants harboring L90M mutation, that is currently under way in our laboratory in cooperation with M. Lepšík.

VII. Conclusions

The aim of this diploma thesis was to identify the relative contributions of the mutations causing lopinavir-resistance phenotype by creating a panel of resistant PR species, based on a highly resistant specimen from a patient. The mutations were introduced into the PR coding region individually or in combination in order to match the ideal "lopinavir mutation score" in the patient, treated by lopinavir for a prolonged period of time.

Individual recombinant PRs were expressed and purified mostly in sufficient amount for crystallization trials. They were enzymatically characterized and their inhibition profiles were analysed with a panel of PIs. K20R and F53L substitutions revealed compensatory effect in the framework of other mutations from lopinavir mutation score and they slightly decrease the level of resistance to lopinavir. Mutation L90M was identified that contributes most significantly to the overall resistant phenotype of the recombinant PR, harbouring all the mutations of the lopinavir mutation score.

We have crystallized the complex of $K4^{K20R,\ F53L}$ HIV-1 protease and lopinavir and the structure was solved and refined at 2.4 Å resolution. The structural studies did not reveal any significant changes compared to that wild-type structure of HIV-1 PR complexed with lopinavir as we expected from the kinetic studies. However, our structure could be used for further computational studies, that can include L90M mutation in calculations. These computations could provide insights into the role of L90M mutation on the overall structure of HIV-1 PR inhibited by lopinavir.

VIII. References

[1] UNAIDS/WHO: AIDS epidemic update, 1-2 (2005): http://www.unaids.org

[2] Barré-Sinoussi, F., Chermann, J.C., Rey, F., Nugeyre, M.T., Chamaret, S., Gruest, J., Dauguet, C., Axler-Blin, C., Vézinet-Brun, F., Rouzinoux, C., Rozenbaum, W. and Montagnier, L.: Science 220, 868-871 (1983)

[3] Gallo, R.C., Sarin, P.S., Gelmann, L.P., Robert-Guroff, M., Richardson, E., Kalyanaraman, V.S., Mann, D., Sidhu, G.D., Stahl, R.E., Zolla-Pazner, S., Leibowitch, J., Popovic, M..: Science 220, 865-867 (1983)

[4] http://arapaho.nsuok.edu/~castillo/NotesImages/Topic159NotesImage1.jpg

[5] Turner, B.G., Summers, M.F.: J. Mol. Biol. 285, 1-32 (1999)

[6] Weiss, R.A.: EMBO reports 4, 10-11 (2003)

[7] Schaeffer, E., Soros, V.B., Greene, W.C.: J.Virol. 78, 1375-1383 (2004)

[8] Jacks, T., Power, M.D., Masiarz, F.R., Luciw, P.A., Baar, P.J. and Varmus, H.E.: Nature 331, 280-283 (1988)

[9] Moulard, M., Decroly, E.: Biochim. Biophys. Acta 1469, 121-132 (2000)

[10] Bukrinskaya, A.G.: Arch. Virol. 149, 1067-1082 (2004)

[11] Gelderblom, H.R.: AIDS 5, 617-638 (1991)

[12] Roebuck, K.A., Saifuddin, M.: Gene Expr. 8, 67-84 (1999)

[13] Larder, B., Richman, D., Vella, S.: HIV resistance and implications for therapy, MediCom Inc., USA (1998)

[14] Trkola, A.: Curr. Opin. Microbiol. 7, 407-411 (2004)

[15] Darke, P.L., Huff, J.R. : Adv. Pharmacol. 25, 399-455 (1994)

[16] Molla, A., Granneman, G.R., Sun, E., Kempf, D.J. : Antiviral Res. 39, 1-23 (1998)

[17] Ratner, R., Haseltine, W., Patarca, R., Livak, K.J., Starcich, B., Josephs, S.F., Doran, E.F., Rafalski, J.A., Whitehorn, E.A., Baumeister, K., Ivanoff, L., Petteway, S.R., Pearson, M.L., Lautenberger, J.A., Papas, T.S., Ghrayeb, J., Chang, N.T., Gallo, R.C. and Wong-Stall, F.: Nature 313, 277-283 (1985)

[18] Navia, M.A., Fitzgerald, P.M.D., McKeever, B.M., Leu, Ch.T., Heimbach, J.C., Herber, W.K., Sigal, I.S., Darke, P.L. and Spriger, J.S.: Nature 337, 615-620 (1989)

[19] Tomasselli, A.G. and Heinrikson, R.L.: Methods Enzymol. Retroviral Proteases 241, 279-301 (1994)

[20] Wlodawer, A., Erickson, J.W. : Annu. Rev. Biochem. 19, 543-585 (1993)

[21] PyMOL ™ 0.98 , DeLano Scientific LLC., http://www.pymol.org/

[22] Stoll, V., Wenying, Q., Kent, D.S., Jacob, C., Chang, P., Walter, K., Simmer, R.L., Helfrich, R., Bussier, D., Kao, J., Kempf, D., Sham, H.L. and Norbeck, D.: Biorganic & Medicinal Cemistry 10, 2803-2806 (2002)

[23] Wlodawer, A., Miller, M., Jaskolski, M., Sathyanarayana, B.K., Baldwin, E., Weber, I.T., Selk, L.M., Clawson, L., Schneider, J., Kent, S. B.: Science *245*, 616-21 (1989)

[24] Wlodawer, A., Vondrasek, J.: Annu. Rev. Biophys. Biomol.Struct. 27, 249-284 (1998)

[25] Prejdova, J., Soucek, M., Konvalinka, J.: Curr.Drug. Targets. Infect. Disord. 4, 137-52 (2004)

[26] Zhang, R.A., Poorman, L.L., Maggiora, R.L., Heinrikson, F.J. and Kezdy, F.: J. Biol. Chem. 266, 15591-15594 (1991)

[27] Flexner, C.: N. Engl. J. Med. 338, 1281-1292 (1998)

[28] U.S. Food and Drug Administration: http://www.fda.gov/oashi/aids/virals.html

[29] Ho, D.D., Toyoshima, T., Mo, H., Kempf, D.J., Norbeck, D, Chen, C.M., Wideburg, N.E., Burt, S.K., Erickson, J.W. and Singh, M.K.: J. Virol. 68, 2016-2020 (1994)

[30] Vacca, J.P., Dorsey, B.D., Schleif, W.A., Levin, R.B., McDaniel, S.L., Darke, P.L., Zugay, J., Quintero, J.C., Blahy, O.M., Roth, E., Sardana, V.V., Schlabach, A.J., Graham, P.I., Condra, J.H., Gotlib, L., Holloway, M.K., Lin, J., Chen, I.-W., Vastag, K., Ostovich, D., Anderson, P.S., Emini, E.A. and Huff, J.R.: Proc. Natl. Acad. Sci. USA 91, 4096-4100 (1994)

[31] Patick, A.K., Mo, H., Markowitz, M., Appelt, K., Wu, B., Musick, L., Kalish, V., Kaldor, S., Reich, S., Ho, D. and Webber, S.: Antimicrob. Agents. Chemother. 40, 292-7 (1996)

[32] Rao, B.G., Kim, E.E., Murcko, M.A.: J. Comput. Aided. Mol. Des. 10, 23-30 (1996)

[33] Furfine, E.S., Baker, C.T., Hale, M.R., Reynolds, D.J., Salisbury, J.A., Searle, A.D., Studenberg, S.D., Todd, D., Tung, R.D. and Spaltenstein, A.: Antimicrob. Agents. Chemother. 48, 791-8 (2004)

[34] Vierling, P. and Greiner, J.: Curr. Pharm. Des. 9, 1755-70 (2003)

[35] Sham, H.L., Kempf, D.J., Molla, A., Marsh, K.C., Kumar, G.N., Chen, C.M., Kati, W., Stewart, K., Lal, R., Hsu, A., Betebenner, D., Korneyeva, M., Vasavanonda, S., McDonald, E., Saldivar, A., Wideburg, N., Chen, X., Niu, P., Park, C., Jayanti, V., Grabowski, B., Granneman, G.R., Sun, E., Japour, A.J., Norbeck, D.W., et al.: Antimicrob. Agents. Chemother. 42, 3218-24 (1998)

[36] Bold, G., Fassler, A., Capraro, H.G., Cozens, R., Klimkait, T., Lazdins, J., Mestan, J., Poncioni, B., Rosel, J., Stover, D., Tintelnot-Blomley, M., Acemoglu, F., Beck, W., Boss, E., Eschbach, M., Hurlimann, T., Masso, E., Roussel, S., Ucci-Stoll, K., Wyss, D., Lang, M.: J. Med. Chem. 41, 3387-401 (1998)

[37] Rusconi, S., La Seta Catamancio, S., Citterio, P., Kurtagic, S., Violin, M., Balotta, C., Moroni, M., Galli, M., d'Arminio-Monforte, A.: Antimicrob. Agents. Chemother. 44, 1328-32 (2000)

[38] Coffin, J.M.: Science 267, 483-489 (1995)

[39] Nijhuis, M., Schuurman, R., de Jong, D., Erickson, J., Gustchina, E., Albert, J., Schipper, P., Gulnik, S., Boucher, C.A.: AIDS 13, 2349-2359 (1999)

[40] Cunningham, S., Ank, B., Lewis, D., Lu, W., Wantman, M., Dileanis, J. A., Jackson, J. B., Palumbo, P., Krogstad, P., Eshleman, S.H.: J. Clin. Microbiol. 39, 1254-7 (2001)

[41] Stuyver, L., Wyseur, A., Rombout, A., Louwagie, J., Scarcez, T., Verhofstede, C., Rimland, D., Schinazi, R.F., Rossau, R.: Antimicrob Agents Chemother, 41, 284-91 (1997)

[42] Larder, B.A., de Vroey, V., Dehertogh, P., Kemp, S., Bloor, S., Hertogs, K.: Antiviral. Ther. 4, 41-42 (1999)

[43] Kellam, P., Larder, B.A.: Antimicorb. Agents. Chemother. 38, 23-30 (1994)

[44] Qari, S.H., Respess, R., Weinstock, H., Beltrami, E.M., Hertogs, K., Larder, B.A., Petropoulos, C.J., Hellmann, N. and Heneine, W.: J. Clin. Microbiol. 40, 31-35 (2002)

[45] Weber, J., Mesters, J.R., Lepsik, M., Prejdova, J., Svec, M., Sponarova, J., Mlcochova, P., Skalicka, K., Strisovsky, K., Uhlikova, T., Soucek, M., Machala, L., Stankova, M., Vondrasek, J., Klimkait, T., Kräusslich, H.-G., Hilgenfeld, R., Konvalinka, J.: J. Mol. Biol. 324, 739-754 (2002)

[46] Erickson, J.W., Burt, S.K.: Annu. Rev. Pharmacol. Toxicol. 36, 545-571 (1996)

[47] Mammano, F., Petit, C., Clavel, F.: J. Virol. 72, 7632-7 (1998)

[48] Maguire, M.F., Guinea, R., Griffin, P., Macmanus, S., Elston, R.C., Wolfram, J., Richards, N., Hanlon, M.H., Porter, D.J., Wrin, T., Parkin, N., Tisdale, M., Furfine, E., Petropoulos, C., Snowden, B.W., Kleim, J.P.: J. Virol. 76, 7398-406 (2002)

[49] Winters, M.A. and Merigan, T.C.: Antimicrob. Agents Chemother. 49, 2575-2582 (2005)

[50] Boden, D., Markowitz, M.: Antimicrob. Agents Chemother. 42, 2775-2783 (1998)

[51] Johnson, V.A., Brun-Vézinet, F., Clotet, B., Conway, B., Kuritzkes, D.R., Pillay, D., Schapiro, J., Telenti, A. and Richman, D.: AIDS-Special Contribution 13, 1 (2005)

[52] Perrin, V. And Mammano, F.: J. Virol. 77, 10172-10174 (2003)

[53] Colonno, R., Rose, R., McLaren, C., Thiry, A., Parkin, N., Friborg, J.: J. Infect. Dis. 189, 1802-10 (2004)

[54] Wlodawer, A.: Annu. Rev. Med. 53, 595-614 (2002)

[55] Cigler, P., Kozisek, M., Rezacova, P., Brynda, J., Otwinowski, Z., Pokorna, J., Plesek, J., Grüner, B., Doleckova-Maresova, L., Masa, M., Sedlacek, J., Bodem, J., Kräusslich, H.G., Kral, V. and Konvalinka, J.: Proc. Natl. Acad. Sci. USA 102, 15394-15399 (2005)

[56] Wlodawer, A.: Curr. Opin. Anti-infect. Investig. Drugs. 1, 246-250 (1999)

[57] Carrillo, A., Stewart, H., Sham, H.L., Norbeck, D.W., Kohlbrenner, W.E., Leonard, J.M., Kempf, D.J. and Molla, A.: J. Virol. 72, 7532-7541 (1998)

[58] Kempf, D.J., Isaacson, J.D., King, M.S., Brun, S.C., Xu, Y., Real, K., Bernstein, B.M., Japour, A.J., Sun, E. and Rode, R.A.: J. Virol. 75, 7462-7469 (2001)

[59] Václavíková, J.: Analysis of drug resistance development in HIV-1 positive patients treated by protease inhibitors: Dissertation thesis, School of Science of the Charles University, Department of Biochemistry, 33 (2004)

[60] Stříšovský, K.: Expression, Isolation and Characterisation of Mutants of HIV-1 Proteinase: Diploma Thesis ICHeT, Prague; Department of Biochemistry and Biotechnology, 29-30 (1997)

[61] Sambrook, J., Fritsch, E.F., Maniatis, T.: Molecular Cloning Laboratory Manual, Cold Spring Harbour Laboratory Press, New York (1989)

[62] QuikChange® Site-Directed Mutagenesis Instruction Manual www.stratagene.com

[63] Studier, F.W., et al.: Methods Enzymol. 85, 60 (1990)

[64] Bradford, M.: Anal. Biochem. 72, 248 (1976)

[65] Richards, A.D., Phylip, L.H., Farmerie, W.G., Scaborough, P.E., Alvarez, A., Dunn, B.M., Hervé-Hirel, P.H., Konvalinka, J., Strop, P., Pavlickova, L., Kostka, V., Kay, J.: J. Biol. Chem. 265, 7733 (1990)

[66] Grafit 5.0.4 http://www.erithacus.com

[67] Urban J., Konvalinka J., Stehlikova J., Gregorova E., Majer P., Soucek M., Andreansky M., Fabry M., Strop P.: FEBS lett. 298, 9-13, (1992)

[68] Williams, J.W., Morrison, J.F. : Methods Enzymol. 63, 437-467 (1979)

[69] Konvalinka, J., Litera, J., Weber, J., Vondrasek, J., Hradilek, M., Soucek, M., Pichova, I., Majer, P., Strop, P., Sedlacek, J., Heuser, A.-M., Kottler, H., Kräusslich, H.-G. : Eur. J. Biochem. 250, 559-566 (1997)

[70] Dixon, M.: Biochem. J. 55, 170-171 (1974)

[71] Jancarik, J. and Kim, S-H.: J. Appl. Cryst. 24, 409-411 (1991)

[72] Ducruix, A. and Giege, R.: Crystallization of nucleic acid and proteins, A practical approach, Oxford University Press, New York 82-86 (1992)

[73] Stura, E.A. and Wilson, I.A.: Methods 1, 38-45 (1990)

[74] Thaller C., Weaver L.H., Eichele G., Karlsson R. And Jansonius J.N.: J. Mol. Biol. 147, 465-469 (1981)

[75] Evans, P.R.: In proceedings of CCP4 Study Weekend on Data Collection and Proceedings, 114-122 (1993)

[76] EPMR 2.5 http://www.msg.ucsf.edu/local/programs/epmr/epmr.html

[77] Murstudov, G.N., Vagin, A.A., Lebedev, A., Wilson, K.S. and Dodson, E.J.: Acta Crystallogr. D55, 247-255 (1999)

[78] Kozisek, M., Prejdova, J., Soucek, M., Machala, L., Stankova, M., Linka, M., Bruckova, M., Konvalinka, J.: Collect. Czech. Chem. Commun. 69, 703-704 (2004)

[79] Gulnik, S.V., Suvorov, L.I., Liu, B., Yu, B., Anderson, B., Mitsuya, H. and Erickson, J.W.: Biochemistry 34, 9282-9287 (1995)

[80] ViewerLite 4.2, Accelrys Inc., http://www.accelrys.com

[81] Ramachandran, G.N. and Sasisekharan, V.: Adv. Protein Chem. 23, 283-438 (1968)

[82] Laskowski, R.A., Mc Arthur, M.W., Moss, D.S., Thorton, J.M.: J. Appl. Cryst. 26, 283-291 (1993)

[83] Miller, M., Geller, M., Gribskov, M., Kent, S.B.H.: Proteins: Struct., Funct., Genet. 27, 184 (1997)

IX: List of Abbreviations

3D	three dimensional
APV	amprenavir
ATV	atanazavir
AZT	azidothymidin (zidovudin)
CA	capsid protein
cDNA	complementary DNA
dATP	deoxyadenosintriphosphate
dCTP	deoxycytidintriphosphate
ddATP	dideoxyadenosintriphosphate
ddCTP	dideoxycytidintriphosphate
ddGTP	dideoxyguanosintriphosphate
ddNTP	dideoxynukleotidtriphosphate
ddTTP	dideoxytymidintriphosphate
dGTP	deoxyguanosintriphosphate
DMSO	dimethysulphoxide
DNA	deoxyribonucleic acid
dTTP	deoxytymidintriphosphate
E. coli	*Escherichia coli*
EDTA	Ethylendiamintetraacetic acid
env	Gene encoding the envelope glycoproteins
EtBr	ethidium bromide
FDA	Food and Drug Administration
FPLC	fast protein liquid chromatography
gag	gene encoding the structural proteins
Gag	polyprotein encoded by *gag*
HAART	highly active antiretroviral therapy
HAPA	hydroxyaminopentane amide
HIV	human immunodeficiency virus
HPLC	high performance liquid chromatography
IC50	concentration of the inhibitor required to inhibit 50%

IDV	indinavir
	Institute of Molecular Genetics
IMG AS CR	Academy of Sciences of the Czech Republic
IN	integrase
	Institute of Organic Chemistry and Biochemistry
IOCB AV CR	Academy of Sciences of the Czech Republic
IPTG	isopropyl-β-D-thiogalactopyranosid
$\mathbf{k_{cat}}$	catalytic rate constant
$\mathbf{K_i}$	inhibition constant
$\mathbf{K_m}$	Michaelis constant
LB	Luria-Bertani medium
LPV	lopinavir
LTR	long terminal repeats
MA	matrix protein
MES	2-(N-morfolin) ethansulfonic acid
mRNA	messenger RNA
MUT	mutant
NC	nucleocapsid protein
NFV	nelfinavir
Nle	norleucin
NMR	nuclear magnetic resonance
Nph	p-nitrophenylalanin
OD	optical density
PAGE	polyacrylamid gel electrophoresis
PEG	polyethylen glycol
PI	protease inhibitor
PMSF	phenylmethylsulphonylfluorid
pol	gene encoding the enzymes of retroviruses
Pol	polyprotein encoded by the *pol* gene
PR	protease
RNA	ribonucleic acid
RNAsa	ribonuclease
RT	reverse transcriptase

RTV	ritonavir
RVA	recombinant viral assay
SDS	sodium dodecylsulphate
SQV	saquinavir
TEMED	N, N, N', N' - tetramethylethylendiamin
TE buffer	Tris-EDTA buffer
TPV	tipranavir
Tris	tris(hydroxymethyl)aminomethan
TSR	template suppression reagent
VdW	Van der Waals
v/v	volume ratio
w/v	weight ratio
wt	wild type

Abbreviation of proteinogenic amino acids consisting of the first three letters of thein names and the single letter symbol:

A	Ala	Alanine	**M**	Met	Methionine
C	Cys	Cysteine	**N**	Asn	Asparagine
D	Asp	Aspartic acid	**P**	Pro	Proline
E	Glu	Glutamic acid	**Q**	Gln	Glutamine
F	Phe	Phenylalanine	**R**	Arg	Arginine
G	Gly	Glycine	**S**	Ser	Serine
H	His	Histidine	**T**	Thr	Threonine
I	Ile	Isoleucine	**V**	Val	Valine
K	Lys	Lysine	**W**	Trp	Tryptophane
L	Leu	Leucine	**Y**	Tyr	Tyrosine

Svoluji k zapůjčení této práce pro studijní účely a prosím, aby byla řádně vedena evidence vypůjčovatelů.

Jméno a příjmení, adresa	Číslo OP	Datum vypůjčení	Poznámka